A CLASS OF FAMILIES OF MAPS WITH HYPERBOLIC HORSESHOES

TORE M. JONASSEN

ABSTRACT. We show that for a class of two-parameter families of mappings $f_{\alpha,\beta} : \mathbb{R}^2 \longrightarrow \mathbb{R}^2$ the bifurcation-set is trapped between two values $\alpha_0(\beta)$ and $\alpha_1(\beta)$ where the non-wandering set $\mathbf{\Omega}(f_\alpha)$ is empty for $\alpha(\beta) < \alpha_0(\beta)$ and the mapping restricted to the non-wandering set is topologically equivalent to a full shift on two symbols for $\alpha(\beta) > \alpha_1(\beta)$. We show that the non-wandering set is a hyperbolic set for some $\alpha_2(\beta) > \alpha_1(\beta)$. Estimates for the parametervalues $\alpha_i(\beta)$ are given in each case. The Hénon mapping is contained in this class. We give several examples of numerical experiments with maps in this class including examples of non-monotone period-doubling bifurcations. In [K&K&Y] it is shown that such bifurcation sequences always occur near non-degenerate homoclinic bifurcations in dissipative plane C^3-diffeomorphisms, but they may be hard to find. At the end we give an example of a two-parameter family (not in the class above) where the non-wandering set consists of three points for $0 \leq \alpha(\beta) < \alpha_0(\beta)$ and where the map restricted to the non-wandering set is topologically equivalent to a full shift on three symbols for $\alpha(\beta) > \alpha_1(\beta)$, and the non-wandering set is hyperbolic for $\alpha(\beta) > \alpha_2(\beta) > \alpha_1(\beta)$. The examples given here will serve as examples in a general theory on smooth systems $x \mapsto f(x)$ lifted to diffeomorphisms by $(x, y) \mapsto (f(x) + \beta y, x)$.

0. A SHORT COMMENT

One aim of this paper is to investigate the relation between a one-dimensional family of maps f_α, and a two-parameter family of plane diffeomorphism $F_{\alpha,\beta}$ constructed from f, by finding explicit bounds in the parameter space of $F_{\alpha,\beta}$ such that $F_{\alpha,\beta}$ has certain properties if (α, β) is in these regions.

Unfortunately this involves lengthy sequences of simple calculations. We have chosen to include these calculations in the proofs, rather than just state the results. Geometrical proofs of the existence of the desired properties in a much larger class of systems will be given elsewhere.

1. NOTATION, DEFINITIONS AND TERMINOLOGY

Non-wandering points. Let $f : M \longrightarrow M$ be a diffeomorphism of a manifold M. A point $p \in M$ is called a non-wandering point for f if, given any neighborhood W of p, there exists some $m > 0$ for which $f^m(W) \cap W \neq \varnothing$. If $p \in M$ is not non-wandering, then it is called wandering. The set of non-wandering points is denoted by $\mathbf{\Omega}(f)$. The set of periodic points is denoted by $\mathbf{Per}(f)$. The set of fixed points is denoted by $\mathbf{Fix}(f)$.

The non-wandering set, $\mathbf{\Omega}(f)$, is closed and f-invariant, and clearly $\mathbf{Fix}(f) \subset \mathbf{Per}(f) \subset \mathbf{\Omega}(f)$. Furthermore $\mathbf{\Omega}(f) = \mathbf{\Omega}(f^{-1})$ and $\mathbf{Per}(f) = \mathbf{Per}(f^{-1})$.

Hyperbolic structure. Let $f : M \longrightarrow M$ be a diffeomorphism of a manifold M. A closed f-invariant set Λ is said to be hyperbolic if there exists a splitting $T_pM = E^s_p \oplus E^u_p$ for each $p \in \Lambda$, which varies continuously with p, a constant $\lambda > 1$ and a Riemannian norm $\|\cdot\|$ such that:

(1) $Df(p)(E^s_p) = E^s_{f(p)}, \quad Df(p)(E^u_p) = E^u_{f(p)}$

(2) $\|Df(p)(v)\| \leq \lambda^{-1}\|v\|$ for $v \in E^s_p, \quad \|Df(p)(v)\| \geq \lambda\|v\|$ for $v \in E^u_p$

Let $T_pM = E^1_p \oplus E^2_p$ be a splitting of the tangent space at p of a Riemannian manifold M. Let $\epsilon : M \longrightarrow \mathbb{R}^+$ be a positive real valued function. By the $\epsilon(p)$-sector $S_{\epsilon(p)}(E^1_p, E^2_p)$ we mean

$$S_{\epsilon(p)}(E^1_p, E^2_p) = \{(v_1, v_2) \in E^1_p \oplus E^2_p : \|v_2\| \leq \epsilon(p)\|v_1\|\}.$$

Key words and phrases. bifurcation, horseshoe, hyperbolic structure, shift-map, numerical experiments.

The complement of $S_{\epsilon(p)}(E^1_p, E^2_p)$ in T_pM is denoted by $S'_{\epsilon(p)}(E^1_p, E^2_p) = T_pM \setminus S_{\epsilon(p)}(E^1_p, E^2_p)$. Let $\lambda > 1$. $Df(p)$ is called a λ-expansion if $\|Df(p)v\| > \lambda\|v\|$ for all $v \in T_pM$.

In this paper $M = \mathbb{R}^2$ and since $T\mathbb{R}^2 = \mathbb{R}^2 \times \mathbb{R}^2$ the Riemannian norm is the usual norm on $T_p\mathbb{R}^2 = \mathbb{R}^2$ induced by the standard inner product. By [New] the following theorem establish conditions for existence of a hyperbolic structure for a f-invariant closed set:

Theorem. *Let f be a C^1-diffeomorphism of a compact Riemannian manifold M, and let $\Lambda \subset M$ be a closed f-invariant set. Then Λ is hyperbolic if and only if there are a splitting $T_pM = E^1_p \oplus E^2_p$ for each $p \in \Lambda$, an integer $m > 0$ a constant $\lambda > 1$ and a positive real valued function $\epsilon : \Lambda \longrightarrow \mathbb{R}^+$ satisfying the following conditions:*

(1) $\sup_{p\in\Lambda} \{\max(\epsilon(p), \epsilon(p)^{-1})\} < \infty$.

(2) For each $p \in \Lambda$ we have $Df^m(p)(S_{\epsilon(p)}) \subset S_{\epsilon(f^m(p))}$.

(3) $Df^m(p)\big|_{S_{\epsilon(p)}}$ and $Df^{-m}(p)\big|_{S'_{\epsilon(p)}}$ are λ-expansions.

By this theorem we need to find a field of cones C_p in T_pM, $p \in \Lambda$, such that $Df(p)$ maps C_p to $C_{f(p)}$ and for some $m > 0$ $Df^m(p)$ expands C_p and $Df^{-m}(p)$ expands $T_pM \setminus C_p$ to establish a hyperbolic structure for a closed f-invariant set Λ. The fields $p \mapsto C_p$ do not have to be continuous. Our manifold $M = \mathbb{R}^2$ is not compact, but this does not matter here because $\mathbb{R}^2$ is flat and we will show that $\Omega(f)$ is contained in a compact set.

Definition of $\widetilde{\mathfrak{G}}^+$, $\mathfrak{G}^+$, $\widetilde{\mathfrak{G}}^-$ and $\mathfrak{G}^-$. $\widetilde{\mathfrak{G}}^+ \subset C^k(\mathbb{R}, \mathbb{R})$, $k \geq 2$, is the subset of maps such that $g \in \widetilde{\mathfrak{G}}^+$ if and only if $g' \in C^{k-1}(\mathbb{R}, \mathbb{R})$ is an order preserving diffeomorphism of $\mathbb{R}$. $\mathfrak{G}^+ \subset \widetilde{\mathfrak{G}}^+$ is the subset with $g(0) = g'(0) = 0$.
$\widetilde{\mathfrak{G}}^- \subset C^k(\mathbb{R}, \mathbb{R})$, $k \geq 2$, is the subset of maps such that $g \in \widetilde{\mathfrak{G}}^-$ if and only if $g' \in C^{k-1}(\mathbb{R}, \mathbb{R})$ is an order reversing diffeomorphism of $\mathbb{R}$. $\mathfrak{G}^- \subset \widetilde{\mathfrak{G}}^-$ is the subset with $g(0) = g'(0) = 0$.

Remark. There is a one-to-one correspondence between $\widetilde{\mathfrak{G}}^+$ and $\widetilde{\mathfrak{G}}^-$ respecting $\mathfrak{G}^+$ and $\mathfrak{G}^-$ defined by $g \mapsto -g$. Let $i : \mathbb{R} \longrightarrow \mathbb{R}$ by $x \mapsto -x$. Then $g \in \mathfrak{G}^+$ if and only if $g \circ i \in \mathfrak{G}^+$ and $g \in \mathfrak{G}^-$ if and only if $g \circ i \in \mathfrak{G}^-$.
If $g \in \widetilde{\mathfrak{G}}^+$ then g has a global minimum in some point $p_m \in \mathbb{R}$, g is strictly decreasing on $(-\infty, p_m]$ and strictly increasing on $[p_m, \infty)$. $g(\mathbb{R}) = [p_m, \infty)$, and g is convex on $\mathbb{R}$. If $g \in \mathfrak{G}^+$ then $p_m = 0$.
If $g \in \widetilde{\mathfrak{G}}^-$ then g has a global maximum in some point $p_m \in \mathbb{R}$, g is strictly increasing on $(-\infty, p_m]$ and strictly decreasing on $[p_m, \infty)$. $g(\mathbb{R}) = [p_m, \infty)$, and g is concave on $\mathbb{R}$. If $g \in \mathfrak{G}^-$ then $p_m = 0$.
$\mathfrak{G}^+$ is "almost closed" under composition in the following sense: Let $f, g \in \mathfrak{G}^+$ and $h = f \circ g$. Then $h'(x) = f'(g(x))g'(x)$. $g(x) > 0$ if $x \neq 0$ so $\operatorname{sign}(h'(x)) = \operatorname{sign}(x)$ since $f'(g(x)) > 0$ if $x \neq 0$ and $g'(x)$ changes sign in $x = 0$. $h''(x) = f''(g(x))(g'(x))^2 + f'(g(x))g''(x) > 0$ if $x \neq 0$ since $f''(g(x)) > 0$, $f'(g(x)) > 0$ and $(g'(x))^2 > 0$ if $x \neq 0$, and $g''(x) > 0$ for all $x \in \mathbb{R}$ by definition of $\mathfrak{G}^+$. Clearly $h''(0) = 0$, so $(h')^{-1}(x)$ exists in all points except $x = 0$. Let $\mathfrak{G}^+ \circ \mathfrak{G}^+ = \{h : h = f \circ g, f, g \in \mathfrak{G}^+\}$. Then $\mathfrak{G}^+ \cap (\mathfrak{G}^+ \circ \mathfrak{G}^+) = \varnothing$, but if we allow $g''(0) = 0$ in $\mathfrak{G}^+$, denoted by $\mathfrak{G}^+_0$, we have $\mathfrak{G}^+_0 \circ \mathfrak{G}^+_0 \subset \mathfrak{G}^+_0$. This also show that $\mathfrak{G}^+$ is primitive in the sense that no member of $\mathfrak{G}^+$ is the composition of two other maps from $\mathfrak{G}^+$.

Definition of $\widetilde{\mathfrak{F}}^+_{\alpha,\beta}, \mathfrak{F}^+_{\alpha,\beta}, \widetilde{\mathfrak{F}}^-_{\alpha,\beta}$ and $\mathfrak{F}^-_{\alpha,\beta}$. $\widetilde{\mathfrak{F}}^+_{\alpha,\beta}$ is the class of families of mappings $f_{g,\alpha,\beta} : \mathbb{R}^2 \longrightarrow \mathbb{R}^2$ defined by the formula

$$f_{g,\alpha,\beta}(x, y) = (\alpha + \beta y - g(x), x)$$

where $g \in \widetilde{\mathfrak{G}}^+$. $\mathfrak{F}^+_{\alpha,\beta} \subset \widetilde{\mathfrak{F}}^+_{\alpha,\beta}$ is the subset with $g \in \mathfrak{G}^+$.
$\widetilde{\mathfrak{F}}^-_{\alpha,\beta}$ is the class of families of mappings $f_{g,\alpha,\beta} : \mathbb{R}^2 \longrightarrow \mathbb{R}^2$ defined by the formula

$$f_{g,\alpha,\beta}(x, y) = (\alpha + \beta y - g(x), x)$$

where $g \in \widetilde{\mathfrak{G}}^-$. $\mathfrak{F}^-_{\alpha,\beta} \subset \widetilde{\mathfrak{F}}^-_{\alpha,\beta}$ is the subset with $g \in \mathfrak{G}^-$.

2. Simple properties of the families $\widetilde{\mathfrak{F}}^+_{\alpha,\beta}, \mathfrak{F}^+_{\alpha,\beta}, \widetilde{\mathfrak{F}}^-_{\alpha,\beta}$ and $\mathfrak{F}^-_{\alpha,\beta}$

We will first establish that all dynamical behavior of the class $\widetilde{\mathfrak{F}}^+_{\alpha,\beta}$ ($\widetilde{\mathfrak{F}}^-_{\alpha,\beta}$) is contained in the class $\mathfrak{F}^+_{\alpha,\beta}$ ($\mathfrak{F}^-_{\alpha,\beta}$). This is done by a simple change of coordinates, and the observation that if $\widetilde{g} \in \widetilde{\mathfrak{G}}^+$ then $g(x) = \widetilde{g}(x + p_m) - \widetilde{g}(p_m)$ is in $\mathfrak{G}^+$. The coordinate transformations in lemma 1, lemma 2 and lemma 4 are all simple, but we do them explicit to show the relations between parameters and maps in the full and reduced classes.

Lemma 1. *Let $\widetilde{f}_{\widetilde{g},\widetilde{\alpha},\widetilde{\beta}} \in \widetilde{\mathfrak{F}}^+_{\alpha,\beta}$ and $f_{g,\alpha,\beta} \in \mathfrak{F}^+_{\alpha,\beta}$ where $g(x) = \widetilde{g}(x + p_m) - \widetilde{g}(p_m)$, $\beta = \widetilde{\beta}$ and $\alpha = \widetilde{\alpha} - (1 - \beta)p_m - \widetilde{g}(p_m)$. Then $\widetilde{f}$ is differentiable equivalent to f.*

Proof. Let $h(x, y) = (x - p_m, y - p_m)$, then $h^{-1}(x, y) = (x + p_m, y + p_m)$.

$$\begin{aligned} h^{-1} \circ f_{g,\alpha,\beta} \circ h(x, y) &= h^{-1} \circ f_{g,\alpha,\beta}(x - p_m, y - p_m) = h^{-1}(\alpha + \beta(y - p_m) - g(x - p_m), x - p_m) \\ &= h^{-1}(\widetilde{\alpha} - \widetilde{g}(p_m) - (1 - \beta)p_m + \widetilde{\beta}(y - p_m) - \widetilde{g}(x + p_m - p_m) + \widetilde{g}(p_m), x - p_m) \\ &= h^{-1}(\widetilde{\alpha} - p_m + \widetilde{\beta}y - \widetilde{g}(x), x - p_m) = (\widetilde{\alpha} + \widetilde{\beta}y - \widetilde{g}(x), x) \\ &= \widetilde{f}_{\widetilde{g},\widetilde{\alpha},\widetilde{\beta}}(x, y) \end{aligned}$$

so $\widetilde{f}$ and f are differentiable conjugate by h since h is differentiable with $Dh = I$. □

We will now establish that all dynamical behavior of the class $\mathfrak{F}^-_{\alpha,\beta}$ is contained in the class $\mathfrak{F}^+_{\alpha,\beta}$. This is again done by a simple change of coordinates. By the remark after the definition of the $\mathfrak{G}$'s we see that if $\widetilde{g} \in \mathfrak{G}^-$ then $g \in \mathfrak{G}^+$ where $g = -\widetilde{g} \circ i$.

Lemma 2. *Let $\widetilde{f}_{\widetilde{g},\widetilde{\alpha},\widetilde{\beta}} \in \mathfrak{F}^-_{\alpha,\beta}$ and $f_{g,\alpha,\beta} \in \mathfrak{F}^+_{\alpha,\beta}$ where $g(x) = -\widetilde{g}(-x)$, $\beta = \widetilde{\beta}$ and $\alpha = -\widetilde{\alpha}$. Then $\widetilde{f}$ is differentiable equivalent to f.*

Proof. Let $h(x, y) = (-x, -y)$, then $h^{-1}(x, y) = (-x, -y)$.

$$\begin{aligned} h^{-1} \circ f_{g,\alpha,\beta} \circ h(x, y) &= h^{-1} \circ f_{g,\alpha,\beta}(-x, -y) = h^{-1}(\alpha - \beta y - g(-x), -x) \\ &= h^{-1}(-\widetilde{\alpha} - \widetilde{\beta} + \widetilde{g}(x), -x) = (\widetilde{\alpha} + \widetilde{\beta}y - \widetilde{g}(x), x) \\ &= \widetilde{f}_{\widetilde{g},\widetilde{\alpha},\widetilde{\beta}}(x, y) \end{aligned}$$

so $\widetilde{f}$ and f are differentiable conjugate by h since h is differentiable with $Dh = -I$. □

Lemma 1 and 2 show that if $f \in \widetilde{\mathfrak{F}}^+_{\alpha,\beta} \cup \widetilde{\mathfrak{F}}^-_{\alpha,\beta}$ we can assume $f_{g,\alpha,\beta} \in \mathfrak{F}^+_{\alpha,\beta}$. The dynamical behavior is preserved by the conjugacies given in the proofs. Furthermore the tangent space structures of orbits and invariant sets are preserved since the conjugacies are linear diffeomorphisms. We will in the following drop the subscript $_{g,\alpha,\beta}$ on $f_{g,\alpha,\beta}$ and simply use f.

Lemma 3. *Let $f \in \mathfrak{F}^+_{\alpha,\beta}$. If $\beta \neq 0$ then f is a diffeomorphism of $\mathbb{R}^2$. If $\beta > 0$ then f is orientation reversing, and if $\beta < 0$ then f is orientation preserving. If $|\beta| < 1$ then f contract area, and if $|\beta| > 1$ then f expand area. If $|\beta| = 1$ then f preserve area.*

Proof. If $\beta \neq 0$ we can solve the equations

$$(v, w) = (\alpha + \beta y - g(x), x)$$

for x and y and any $g : \mathbb{R} \longrightarrow \mathbb{R}$. We find

$$\begin{aligned} x &= w \\ y &= \frac{1}{\beta}(v - \alpha + g(w)) \end{aligned}$$

and hence

$$f^{-1}(x,y) = \left(y, \beta^{-1}(x - \alpha + g(y))\right).$$

Both f and f^{-1} are smooth, and

$$Df(x,y) = \begin{bmatrix} -g'(x) & \beta \\ 1 & 0 \end{bmatrix}$$

so $\det(Df(x,y)) = -\beta$. The equation $\det(Df(x,y)) = -\beta$ implies the rest of the statements in lemma 3. □

The next lemma shows that a subclass $\mathfrak{f}^+_{\alpha,\beta} \subset \mathfrak{F}^+_{\alpha,\beta}$ contains maps displaying all possible dynamical behavior in $\mathfrak{F}^+_{\alpha,\beta}$. There are several choices for the subclass $\mathfrak{f}^+_{\alpha,\beta}$, but the natural choice is given by

$$\mathfrak{f}^+_{\alpha,\beta} = \{f_{\alpha,\beta,g} \in \mathfrak{F}^+_{\alpha,\beta} : |\beta| \leq 1\}.$$

The reason for this particular choice will become clear later. Let

$$\widetilde{\mathfrak{f}}^+_{\alpha,\beta} = \{f_{\alpha,\beta,g} \in \mathfrak{F}^+_{\alpha,\beta} : 0 < |\beta| \leq 1\}.$$

Lemma 4 establish a differentiable equivalence between maps in $\widetilde{\mathfrak{f}}^+_{\alpha,\beta}$ and inverses of maps in $\mathfrak{F}^+_{\alpha,\beta} \setminus \mathfrak{f}^+_{\alpha,\beta}$.

Lemma 4. *Let $f \in \mathfrak{F}^+_{\alpha,\beta}$, $f(x,y) = (\alpha + \beta y - g(x), x)$ with $\beta \neq 0$. Then f^{-1} is differentiable equivalent to $\widetilde{f} \in \mathfrak{F}^+_{\alpha,\beta}$ given by $\widetilde{f}(x,y) = (\alpha + \widetilde{\beta} y - g(-\widetilde{\beta} x), x)$ where $\widetilde{\beta} = 1/\beta$.*

Proof. Suppose $\beta \neq 0$ and define $k(x) = g\left(-\frac{x}{\beta}\right)$. Then $k \in \mathfrak{G}^+$ if and only if $g \in \mathfrak{G}^+$. Let $h(x,y) = (-\beta y, -\beta x)$. Then $h^{-1}(x,y) = (-y/\beta, -x/\beta)$ and h is a linear diffeomorphism. We find

$$\begin{aligned} h \circ f^{-1} \circ h^{-1}(x,y) &= h \circ f^{-1}(-y/\beta, -x/\beta) = h(-\beta^{-1}x, \beta^{-1}(-\beta^{-1}y - \alpha + g(-\beta^{-1}x))) \\ &= (-\beta\beta^{-1}(-\beta^{-1}y - \alpha + g(-\beta^{-1}x)), -(-\beta)\beta^{-1}x) = (\alpha + \beta^{-1}y - g(-\beta^{-1}x), x) \\ &= (\alpha + \widetilde{\beta} y - g(-\widetilde{\beta} x), x) = \widetilde{f}(x,y). \end{aligned}$$

□

Let $f \in \mathfrak{F}^+_{\alpha,\beta} \setminus \mathfrak{f}^+_{\alpha,\beta}$, $\widetilde{f} \in \widetilde{\mathfrak{f}}^+_{\alpha,\beta}$ and h be as in lemma 4. Lemma 4 establish a differentiable equivalence of f^{-1} and $\widetilde{f}$, so $\widetilde{f}$ reflects the dynamics of f. To be precise the dynamics of f is obtained from the dynamics of $\widetilde{f}$ in the following way:
By lemma 4 and the properties of periodic points and the non-wandering set we have $h^{-1}(\mathbf{Per}(\widetilde{f}) = \mathbf{Per}(f^{-1}) = \mathbf{Per}(f)$ and $h^{-1}(\mathbf{\Omega}(\widetilde{f}) = \mathbf{\Omega}(f^{-1}) = \mathbf{\Omega}(f)$. Hence $\mathbf{Per}(\widetilde{f})$ and $\mathbf{Per}(f)$, and $\mathbf{\Omega}(\widetilde{f})$ and $\mathbf{\Omega}(f)$ are diffeomorphic. Let Λ be a hyperbolic invariant set of $\widetilde{f}$ with stable manifolds $W^s(p,\widetilde{f})$ and unstable manifolds $W^u(p,\widetilde{f})$, $p \in \Lambda$. This structure is diffeomorphically carried over to the f-invariant set $h^{-1}(\Lambda)$ and therefore

$$\begin{aligned} h^{-1}(W^s(p,\widetilde{f}) &= W^s(h^{-1}(p), f^{-1}) = W^u(h^{-1}(p), f) \\ h^{-1}(W^u(p,\widetilde{f}) &= W^u(h^{-1}(p), f^{-1}) = W^s(h^{-1}(p), f). \end{aligned}$$

If p is a periodic point of $\widetilde{f}$ with a center manifold $W^c(p,\widetilde{f})$ then $h^{-1}(W^c(p,\widetilde{f}) = W^c(h^{-1}(p), f^{-1}) = W^c(h^{-1}(p), f)$.
In particular, attractors of $\widetilde{f}$ becomes repellors of f, and hyperbolic saddles of $\widetilde{f}$ are hyperbolic saddles of f with the stable and unstable manifold interchanged.

In view of lemma 1, lemma 2 and lemma 4 we will in the following only be concerned with the class $\mathfrak{f}^+_{\alpha,\beta}$. All results may then be translated to the class $\widetilde{\mathfrak{F}}^+_{\alpha,\beta} \cup \widetilde{\mathfrak{F}}^-_{\alpha,\beta}$ using the equivalences above.

3. Simple properties of the families of maps in $\mathfrak{f}^+_{\alpha,\beta}$.

Let $f \in \mathfrak{f}^+_{\alpha,\beta}$, then by lemma 3, f is area contracting and orientation reversing diffeomorphism if $0 < \beta < 1$, area preserving and orientation reversing diffeomorphism if $\beta = 1$, area contracting and orientation preserving diffeomorphism if $-1 < \beta < 0$ and area preserving and orientation preserving diffeomorphism if $\beta = -1$. If $\beta = 0$ then f is not a diffeomorphism.

Let H_{y_0} be the horizontal line defined by $H_{y_0} = \{(x, y) \in \mathbb{R}^2 : x \in \mathbb{R} \text{ and } y = y_0\}$, and V_{x_0} be the vertical line defined by $V_{x_0} = \{(x, y) \in \mathbb{R}^2 : x = x_0 \text{ and } y \in \mathbb{R}\}$. We define the following class of curves in $\mathbb{R}^2$ by

$$C(a, b, g) = \{(x, y) \in \mathbb{R}^2 : x = a - g(t), y = t, t \in \mathbb{R}\}$$
$$\widehat{C}(a, b, g) = \{(x, y) \in \mathbb{R}^2 : x = t, y = \frac{1}{b}(g(t) - a), t \in \mathbb{R}\}$$

where $\widehat{C}(a, b, g)$ is undefined for $b = 0$.

FIGURE 1.1.
The sequence of images $\widehat{C}(\gamma, \beta, g) \xrightarrow{f} V_{\alpha-\gamma} \xrightarrow{f} H_{\alpha-\gamma} \xrightarrow{f} C((1+\beta)\alpha - \beta\gamma, \beta, g)$ for $\gamma = 0$, $\alpha = 1$, $\beta = 1/2$ and $g(x) = x^2$.

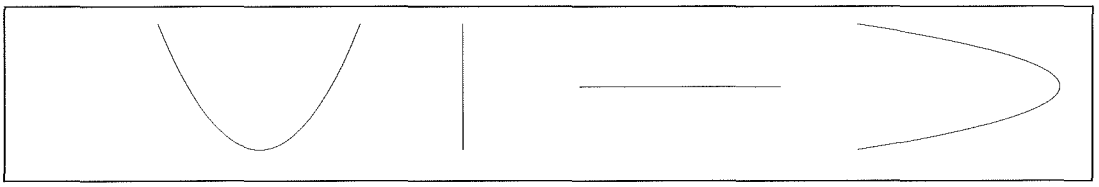

Let $f \in \mathfrak{f}^+_{\alpha,0}$. Then $f(H_{y_0}) = C(\alpha, 0, g)$ for all $y_0 \in \mathbb{R}$ and $f(V_{x_0}) = (\alpha - g(x_0), x_0)$. Hence $f(\mathbb{R}^2) = C(\alpha, 0, g)$, $f(C(\alpha, 0, g)) = C(\alpha, 0, g)$ and $\mathbf{\Omega}(f) \subset C(\alpha, 0, g)$, and the dynamics of f on $C(\alpha, 0, g)$ is induced by the one-dimensional map $x \mapsto \alpha - g(x)$.

Let $f \in \mathfrak{f}^+_{\alpha,\beta}$ with $\beta \neq 0$. Then $f(H_{y_0}) = C(\alpha + \beta y_0, \beta, g)$, $f(V_{x_0}) = H_{x_0}$, $f^{-1}(H_{y_0}) = V_{y_0}$ and $f^{-1}(V_{x_0}) = \widehat{C}(\alpha - x_0, \beta, g)$. From these equations and the fact that f is a diffeomorphism we obtain

$$f(\widehat{C}(\alpha - x_0, \beta, g)) = V_{x_0}$$
$$f^2(\widehat{C}(\alpha - x_0, \beta, g)) = f(V_{x_0}) = H_{x_0}$$
$$f^3(\widehat{C}(\alpha - x_0, \beta, g)) = f^2(V_{x_0}) = f(H_{x_0}) = C(\alpha + \beta x_0, \beta, g).$$

From the above we obtain the following two sequences of images illustrating the geometry in the map:

$$\widehat{C}(\gamma, \beta, g) \xrightarrow{f} V_{\alpha-\gamma} \xrightarrow{f} H_{\alpha-\gamma} \xrightarrow{f} C((1+\beta)\alpha - \beta\gamma, \beta, g)$$
$$C(\gamma, \beta, g) \xrightarrow{f^{-1}} H_{\frac{\gamma-\alpha}{\beta}} \xrightarrow{f^{-1}} V_{\frac{\gamma-\alpha}{\beta}} \xrightarrow{f^{-1}} \widehat{C}(\frac{1}{\beta}((1+\beta)\alpha - \gamma), \beta, g).$$

These sequences of images are illustrated in figure 1.1 for a typical map in $\mathfrak{f}^+_{\alpha,\beta}$, $\beta \neq 0$.

4. Maps with empty non-wandering set

Let $f \in \mathfrak{f}^+_{\alpha,\beta}$. We will prove that the non-wandering set is empty for all $\alpha(\beta) < \alpha_0(\beta)$ for some $\alpha_0(\beta)$. Let π_i denote projection on the i-th component, $\pi_i(x_1, x_2) = x_i$, $i = 1, 2$, and let Δ denote the diagonal in $\mathbb{R}^2$.

FIGURE 1.2.
Left: The y-axis is mapped to the x-axis, and the x-axis is mapped to the g-shaped curve. **Right:** The x-axis is mapped to the y-axis, and the y-axis is mapped to a g-shaped curve by the inverse map. In both cases $\alpha = -\frac{1}{8}$, $\beta = -\frac{1}{2}$ and $g(x) = \cosh(x) - 1$.

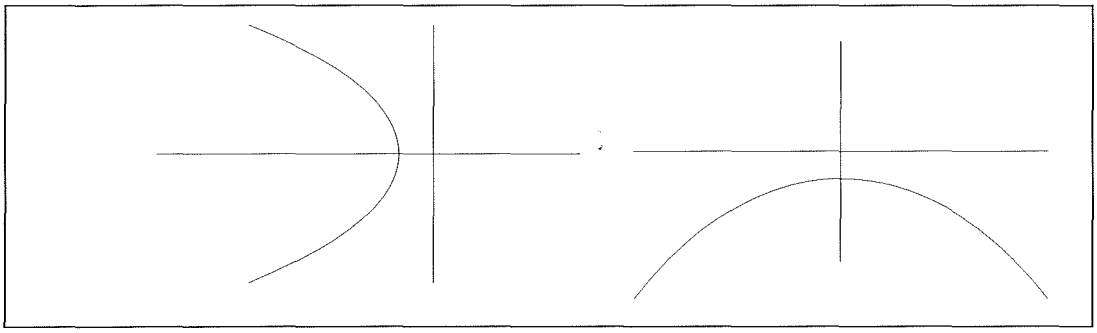

Lemma 5. *Suppose $f : \mathbb{R}^2 \longrightarrow \mathbb{R}^2$ is a continuous map and $K \subset \mathbb{R}^2$ is a closed subset such that* int $K \neq \varnothing$ *and $f(K) \subset$ int K. Suppose $\pi_i \circ f(p) < \pi_i(p)$ $(\pi_i \circ f(p) > \pi_i(p))$, $i = 1$ or $i = 2$, for every $p \in$ int K. Then $\mathbf{\Omega}(f) \cap$ int $K = \varnothing$.*

Remark. The subset K can not be a bounded subset, else f would have a fixed point in K by Brouwers fixed point theorem. An analogous result may of course be formulated for one dimensional maps, but we refer to lemma 5 also in the one dimensional case.

Proof. Let $p \in$ int K. It is easily seen that there exists $\epsilon > 0$ such that the image of the ϵ-ball of p does not intersect the ϵ-ball of p. Clearly the image of p under iterations by f does not return to a vertical strip of size 2ϵ of p. □

Lemma 6. *Suppose $f \in \mathfrak{f}^+_{\alpha,\beta}$. Then $f(\Delta) \cap \Delta = \mathbf{Fix}(f)$.*

Proof. Suppose $p \in f(\Delta) \cap \Delta$. Then $(s, s) = (\alpha + \beta t - g(t), t)$ so $s = t$. Hence $(s, s) \mapsto (\alpha + \beta s - g(s), s) = (s, s)$, so $p = (s, s) \in \mathbf{Fix}(f)$.
Suppose $p \in \mathbf{Fix}(f)$. Then $(s, t) = (\alpha + \beta t - g(s), s)$, so $s = t$, and $p = (s, t) = (s, s) \in \Delta$. Since $p = f(p)$ we see that $p \in f(\Delta)$ so $p \in f(\Delta) \cap \Delta$. □

Lemma 7. *Suppose $f \in \mathfrak{f}^+_{\alpha,\beta}$. Then $\mathbf{\Omega}(f) \neq \varnothing$ if and only if $\mathbf{Fix}(f) \neq \varnothing$.*

Proof. The if part is trivial since $\mathbf{Fix}(f) \subset \mathbf{\Omega}(f)$.
It is a well known fact that for any orientation preserving homeomorphism of the plane then the non-wanderingset is empty if the fixed point set is empty ([A1] and [A2]). We will however give elementary proofs in the cases $\beta \leq 0$.
Suppose $\beta = 0$. Consider $x \mapsto \alpha - g(x)$. Then $\mathbf{Fix}(\alpha - g(x)) = \varnothing$ implies $\alpha - g(x) < x$ for all $x \in \mathbb{R}$. Then by lemma 5 $\mathbf{\Omega}(\alpha - g(x)) = \varnothing$ and hence $\mathbf{\Omega}(f) = \varnothing$.
Suppose $\beta < 0$. Let $\mathbb{R}^2 \setminus \Delta = S_1 \cup S_2$, where S_1 denotes the connected component containing the negative x-axis, and S_2 denotes the connected component containing the positive x-axis. Suppose $\mathbf{Fix}(f) = \varnothing$. By the geometric properties of f in section 2 and lemma 6 we see that $f(S_1) \subset S_1$ and $f^{-1}(S_2) \subset S_2$, and that the inclusions are strict. Let $p_0 = (x_0, y_0) \in S_1$, and consider the vertical linesegment $V_{x_0} = \{x_0\} \times [x_0, \infty) \subset S_1$. Clearly $p_0 \in V_{x_0}$. We see that $f(V_{x_0})$ is a horizontal linesegment, and $\pi_1(f(p_0)) < \max \pi_1(f(V_{x_0})) < x_0 = \pi_1(p_0)$. Then by lemma 5 $\mathbf{\Omega}(f) \cap S_1 = \varnothing$. Similarly, let $p_0 = (x_0, y_0) \in S_2$, and consider the horizontal linesegment $H_{y_0} = [y_0, \infty) \times \{y_0\}$. Clearly $p_0 \in H_{y_0}$. We see that $f^{-1}(H_{y_0})$ is a vertical linesegment, and $\pi_2(f(p_0)) < \max \pi_2(f^{-1}(V_{y_0})) < y_0 = \pi_2(p_0)$. Then by lemma 5, $\mathbf{\Omega}(f) \cap S_2 = \varnothing$. Hence $\mathbf{\Omega}(f) = \varnothing$.
Suppose $\beta > 0$. The direct method above does not apply to this case, and f is orientation reversing so the result cited above does not apply directly. However, by the remark above it is sufficient to show that $\mathbf{Fix}(f) = \varnothing$ implies that there are no period 2 points, since we may replace f by f^2 to obtain a

orientation preserving map. By the formulas for f and f^{-1} we find that f^2 has a fixed point if and only if the set of equations $g(x)+(1-\beta)y-\alpha=0$ and $g(y)+(1-\beta)x-\alpha=0$ has solutions. It is clear that if one of the curves intersect Δ then the other curve intersect Δ in the same point, and this point satisfy the fixed point equation for f. It is also clear, by writing the two curves as $y=(1-\beta)^{-1}(\alpha-g(x))$ and $x=(1-\beta)^{-1}(\alpha-g(y))$, that the two curves can not intersect without intersecting Δ, which proves that $\mathbf{Fix}(f)=\varnothing$ implies $\mathbf{Fix}(f^2)=\varnothing$, and hence by [A2] $\mathbf{\Omega}(f^2)=\mathbf{\Omega}(f)=\varnothing$. □

Theorem 1. *Suppose $f\in \mathfrak{f}^+_{\alpha,\beta}$ where $f(x,y)=(\alpha+\beta y-g(x),x)$. Then $\mathbf{\Omega}(f)=\varnothing$ if and only if $\alpha(\beta)<\alpha_0(\beta)$ where $\alpha_0(\beta)$ is given by $\alpha_0(\beta)=g((g')^{-1}(\beta-1))-(\beta-1)(g')^{-1}(\beta-1)$.*

Proof. By lemma 7 we only need to find the parametervalue where the first fixed point appear. From the formula for f we see that f has fixed points if and only if $\alpha+\beta x-g(x)=x$ has solutions. This equation has exactly one solution x_0 if and only if $g'(x_0)+(1-\beta)=0$. Since g' is invertible we get $x_0=(g')^{-1}(\beta-1)$. The fixed point equation now gives the formula for $\alpha_0(\beta)$, and it is easy to see that the equation has no solutions for $\alpha(\beta)<\alpha_0(\beta)$ and two solutions if $\alpha(\beta)>\alpha_0(\beta)$. □

5. Approximate location of the non-wandering set

Theorem 2. *Given $f\in \mathfrak{f}^+_{\alpha,\beta}$ by $f(x,y)=f_{\alpha,\beta}(x,y)=(\alpha+\beta y-g(x),x)$, α,β fixed. Let $h_1(x)=g(x)+(1+|\beta|)x-\alpha$ and $h_2(x)=g(x)-(1+|\beta|)x-\alpha$. Let $\mathcal{S}_i$ denote the set of solutions of $h_i=0$, $i=1,2$, and let $\mathcal{S}=\mathcal{S}_1\cup\mathcal{S}_2$. If $\mathcal{S}=\varnothing$ then $\mathbf{\Omega}(f)=\varnothing$. Suppose $\mathcal{S}\neq\varnothing$. Let $R_m=\max_{x_0\in\mathcal{S}}\{|x_0|\}$ and let $R>R_m$. Then $\mathbf{\Omega}(f)\subset \operatorname{int}([-R,R]\times[-R,R])$.*

Proof. Let Δ^+ denote the diagonal and Δ^- denote the antidiagonal in $\mathbb{R}^2$. $f(\Delta^+)$ and $f(\Delta^-)$, the images of Δ^+ and Δ^- under f, are given in parametric form by

$$\begin{aligned} F_1:&\quad t\mapsto(\alpha+\beta t-g(t),t)\\ F_2:&\quad t\mapsto(\alpha-\beta t-g(t),t)\end{aligned}$$

$\pi_1\circ F_1(t)$ obtain its maximum at $t=(g')^{-1}(\beta)$ and $\pi_1\circ F_2(t)$ obtain its maximum at $t=(g')^{-1}(-\beta)$. The two curves intersect at $(\alpha,0)$, the image of $(0,0)$. The points in $f(\Delta^+)\cap\Delta^+$ and $f(\Delta^-)\cap\Delta^+$ are found by solving the equations $\pi_1\circ F_i(t)=t$, $i=1,2$, and the points in $f(\Delta^+)\cap\Delta^-$ and $f(\Delta^-)\cap\Delta^-$ are found by solving the equations $\pi_1\circ F_i(t)=-t$, $i=1,2$. We note that each intersection consists of at most two points. The relevant intersections are in the left half-plane, so since $\pi_1\circ(F_1-F_2)(t)=2\beta t$ and $\pi_2\circ(F_1-F_2)(t)=0$, $\pi_2\circ F_2=t$ give the larger norm of the root in the lower left half-plane, and $\pi_2\circ F_1=-t$ give the larger norm of the root in the upper left half-plane if $\beta>0$. If $\beta<0$ $\pi_2\circ F_1=t$ give the larger norm of the root in the lower left half-plane, and $\pi_2\circ F_2=-t$ give the larger norm of the root in the upper left half-plane. The relevant equations are $g(t)\pm(1+\beta)t-\alpha=0$ if $\beta>0$ and $g(t)\pm(1-\beta)t-\alpha=0$ if $\beta<0$.

By considering $f^{-1}(\Delta^+)$ and $f^{-1}(\Delta^-)$ given in parametric form by

$$\begin{aligned} G_1:&\quad t\mapsto(t,\beta^{-1}(g(t)+t-\alpha))\\ G_2:&\quad t\mapsto(t,\beta^{-1}(g(t)-t-\alpha))\end{aligned}$$

The points in $f^{-1}(\Delta^+)\cap\Delta^+$ and $f^{-1}(\Delta^-)\cap\Delta^+$ are found by solving the equations $\pi_2\circ G_i(t)=t$, $i=1,2$, and the points in $f^{-1}(\Delta^+)\cap\Delta^-$ and $f^{-1}(\Delta^-)\cap\Delta^-$ are found by solving the equations $\pi_2\circ G_i(t)=-t$, $i=1,2$. It is easily seen that this is the same set of equations as $\pi_i\circ F_i(t)=\pm t$, $i=1,2$. The relevant intersections are in the upper half-plane if $\beta>0$ and in the lower half-plane if $\beta<0$, so since $\pi_2\circ(G_1-G_2)(t)=2\beta^{-1}t$ and $\pi_1\circ(G_1-G_2)(t)=0$, $\pi_1\circ G_2=\pm t$ and $\pi_2\circ G_1=-t$ give the larger norm of the roots. The relevant equations are $g(t)+(1+\beta)t-\alpha=0$ and $g(t)-(1-\beta)t-\alpha=0$.

FIGURE 1.3.
The figure shows parts of Δ^+, Δ^-, and parts of the curves F_1 and F_2 for a typical map in $\mathfrak{f}^+_{\alpha,\beta}$. The map used in this example is given by $(x,y) \mapsto (\alpha + \beta y - g(x), x)$ where $\alpha = 2$, $\beta = 1/3$ and $g(x) = 2(\cosh(x) - 1)$ if $x < 0$ and $g(x) = x^2$ if $x \geq 0$.

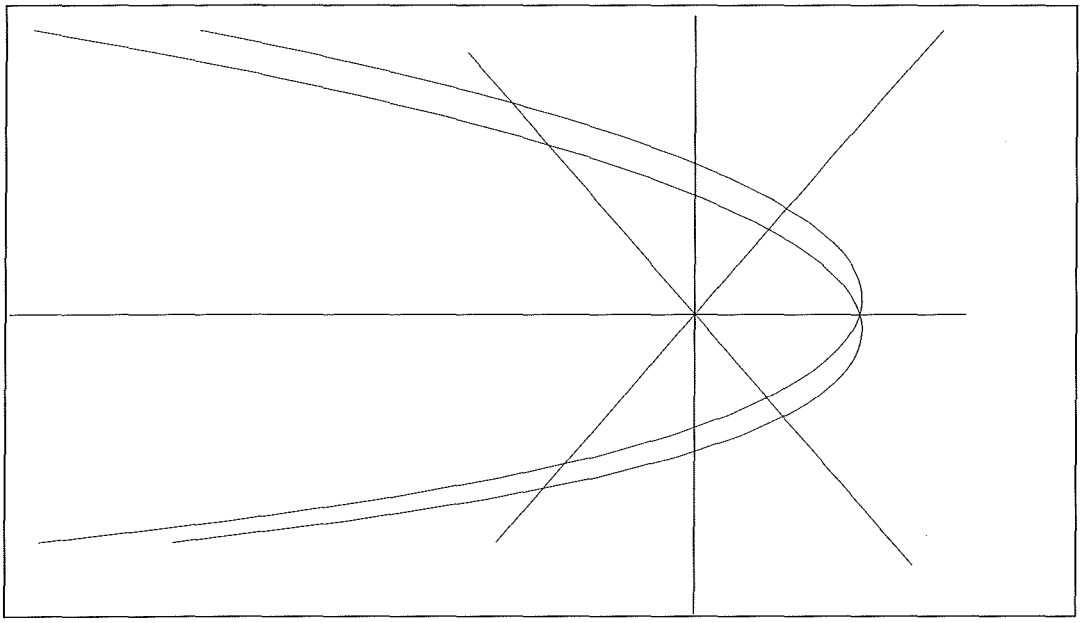

We need only to consider the equations which give the larger norm of the roots, and it is easily seen that it is sufficient to consider the equations $\alpha \pm (1 + |\beta|)t - g(t) = 0$ from the set of equations above.

Let $h_1(x) = g(x) + (1 + |\beta|)x - \alpha$ and $h_2(x) = g(x) - (1 + |\beta|)x - \alpha$. Let $\mathcal{S}_i$ denote the set of solutions of $h_i = 0$, $i = 1, 2$, and let $\mathcal{S} = \mathcal{S}_1 \cup \mathcal{S}_2$. Suppose $\mathcal{S} \neq \varnothing$. Let $R_m = \max_{x_0 \in \mathcal{S}}\{|x_0|\}$ and let $R > R_m$. Let $M_1(R) = \{(x,y) \in \mathbb{R}^2 : x \leq -|y|, x \leq -R\}$, $M_2(R) = \{(x,y) \in \mathbb{R}^2 : x \geq |y|, x \geq R\}$, $M_3(R) = \{(x,y) \in \mathbb{R}^2 : y \leq -|x|, y \leq -R\}$ and $M_4(R) = \{(x,y) \in \mathbb{R}^2 : y \geq |x|, y \geq R\}$. By the above $f(\partial M_i(R)) \cap \Delta^+ = \varnothing$, $f(\partial M_i(R)) \cap \Delta^- = \varnothing$, $i = 1, 2$, and $f^{-1}(\partial M_j(R)) \cap \Delta^+ = \varnothing$, $f^{-1}(\partial M_j(R)) \cap \Delta^- = \varnothing$, $j = 3, 4$. We see by the geometric properties of f that $f(M_1(R) \cup M_2(R)) \subset \text{int } M_1(R)$, and $f^{-1}(M_3(R) \cup M_4(R)) \subset \text{int } M_4(R)$ if $\beta > 0$ and $f^{-1}(M_3(R) \cup M_4(R)) \subset \text{int } M_3(R)$ if $\beta < 0$. By lemma 5 as in the proof of lemma 7 we see that $\mathbf{\Omega}(f) \cap (M_1(R) \cup M_2(R) \cup M_3(R) \cup M_4(R)) = \varnothing$ so $\mathbf{\Omega}(f) \subset \mathbb{R}^2 \setminus (M_1(R) \cup M_2(R) \cup M_3(R) \cup M_4(R)) = \text{int } ([-R, R] \times [-R, R])$.

If $\beta = 0$ it is easily seen that $\mathbf{\Omega}(f) = \varnothing$ if $\alpha - g(x) < x$, and that $\mathbf{\Omega}(\alpha - g(x))$ is contained in the interval $[a, b]$ where a is the smallest solution of $\alpha - g(x) = x$ and b is the largest solution of $\alpha - g(x) = -x$. In particular the formulas in the theorem apply. If $\mathcal{S} = \varnothing$ let $R = 0$. Then $M_1(0) \cup M_2(0) \cup M_3(0) \cup M_3(0) = \mathbb{R}^2$ so $\mathbf{\Omega}(f) = \varnothing$ by the arguments above. □

6. MAPS WITH TOPOLOGICAL HORSESHOES

Theorem 3. *Suppose $f \in \mathfrak{f}^+_{\alpha,\beta}$ where $f(x,y) = (\alpha + \beta y - g(x), x)$. Let $r(R) = \min\{g(-R) - (|\beta| + 1)R, g(R) - (|\beta|+1)R\}$ and $l(R) = (|\beta|+1)R$. Let R_h be the unique point in the set $\{R : l(R) = r(R), R > 0\}$, and let $\alpha_1(\beta) = l(R_h)$. For every $\alpha(\beta) > \alpha_1(\beta)$ there is a homeomorphism $h_{\alpha(\beta)} : \mathbf{\Omega}(f) \longrightarrow \Sigma_2$ such that the restriction $f : \mathbf{\Omega}(f) \longrightarrow \mathbf{\Omega}(f)$ is topological equivalent to the shiftmap $\sigma : \Sigma_2 \longrightarrow \Sigma_2$.*

Proof. Let $R > 0$ and let $\mathcal{S}(R)$ denote the closed square with vertices $p_1 = (-R, -R)$, $p_2 = (R, -R)$, $p_3 = (R, R)$ and $p_4 = (-R, R)$. Let $\mathcal{L}_i(R)$ denote the linesegments with endpoints p_i and $p_{i+1 \bmod 4}$, $i = 1, \ldots, 4$. $\partial f(\mathcal{S}(R)) = f(\mathcal{L}_1(R)) \cup \cdots f(\mathcal{L}_4(R))$ where $f(\mathcal{L}_1(R))$ and $f(\mathcal{L}_3(R))$ are g-shaped curves, and $f(\mathcal{L}_2(R))$ and $f(\mathcal{L}_4(R))$ are horizontal linesegments. Clearly $\max \pi_1(f(\mathcal{L}_1(R))) = \pi_1(f(0, -R)) = \alpha - \beta R$,

$\max \pi_1(f(\mathcal{L}_3(R))) = \pi_1(f(0,R)) = \alpha + \beta R$, $\pi_2(f(\mathcal{L}_2(R)) = R$ and $\pi_2(f(\mathcal{L}_4(R))) = -R$. Furthermore $\max \pi_1(f(\mathcal{L}_2(R))) = \alpha+\beta R-g(R)$, $\max \pi_1(f(\mathcal{L}_4(R))) = \alpha+\beta R-g(-R)$ and $\pi_1(f(0,R)) > \pi_1(f(0,-R))$ if $\beta > 0$, and $\max \pi_1(f(\mathcal{L}_2(R))) = \alpha-\beta R-g(R)$, $\max \pi_1(f(\mathcal{L}_4(R))) = \alpha-\beta R-g(-R)$ and $\pi_1(f(0,R)) < \pi_1(f(0,-R))$ if $\beta < 0$.

$f(\mathcal{S}(R)) \cap \mathcal{S}(R)$ consists of two horizontal strips cutting completely thorough $\mathcal{S}(R)$ if

$$\min\{\max \pi_1(f(\mathcal{L}_1(R))), \max \pi_1(f(\mathcal{L}_3(R)))\} > R$$
$$\max\{\max \pi_1(f(\mathcal{L}_2(R))), \max \pi_1(f(\mathcal{L}_4(R)))\} < -R.$$

In terms of α, β, g and R these conditions take the form

$$\begin{aligned} \alpha - |\beta|R &> R \\ \max\{\alpha + |\beta|R - g(R), \alpha + |\beta|R - g(-R)\} &< -R. \end{aligned} \tag{1}$$

We see that

$$\begin{aligned} &\max\{\alpha + |\beta|R - g(R), \alpha + |\beta|R - g(-R)\} = \alpha + |\beta|R + \max\{-g(R), -g(-R)\} \\ &= \alpha + |\beta|R - \min\{g(R), g(-R)\} = \alpha + |\beta|R - h(R), \end{aligned}$$

where $h(R) = \min\{g(R), g(-R)\}$. Then the conditions (1) takes the form

$$\begin{aligned} \alpha &> (1 + |\beta|)R \\ \alpha &< h(R) - (1 + |\beta|)R. \end{aligned}$$

The properties of g implies that $h(R)$ is an increasing piece-wise smooth for $R \geq 0$, and the curve $h(R)-(1+|\beta|)R$ intersect the line $(1+|\beta|)R$ in exactly two points for $R \geq 0$, $R = 0$ and $R(\beta) = R_1(\beta) > 0$. Therefore the inequalities $(1+|\beta|)R < \alpha < h(R)-(1+|\beta|)R$ defines a sector $\mathcal{M}_\beta$ in the $R\alpha$-plane bounded by the curves $(1 + ||\beta)R$ and $h(R) - (1 + |\beta|)R$ for $R > R_1$. For any $\alpha(\beta) > \alpha_1(\beta) = (1 + |\beta|)R_1(\beta)$, where R_1 is the positive solution of $2(1 - |\beta|)R = h(R)$, we can find a R such that (1) holds. To be precise, given $\alpha(\beta) > \alpha_1(\beta)$ the condition (1) holds if $R \in (R_l, R_r)$ where R_l is the positive solution of $\alpha(\beta) = h(R)-(1+|\beta|)R$ and R_r is the solution of $\alpha(\beta) = (1+|\beta|)R$, given by $R_r = \alpha(\beta)/(1+|\beta|)$. Since $h(R) = \min\{g(R), g(-R)\}$ it is easily seen that the conditions of theorem 2 is satisfied if R is chosen as above. Hence $\mathbf{\Omega}(f) \subset \mathcal{S}(R)$.

The preimage of $\mathcal{S} \cap f(\mathcal{S})$, $f^{-1}(\mathcal{S} \cap f(\mathcal{S})) = f^{-1}(\mathcal{S}) \cap \mathcal{S}$, consists of two vertical strips cutting completely through $\mathcal{S}$. Using the standard definitions of horizontal and vertical strips bounded by curves as in [G&H], we see that the image of a horizontal strip gives two horizontal strips in $\mathcal{S}$, and the preimage of a vertical strip give two vertical strips in $\mathcal{S}$. Hence

$$H_n = \bigcap_{i=0}^{n} f^i(\mathcal{S}) \text{ and } V_n = \bigcap_{i=0}^{n} f^{-i}(\mathcal{S})$$

consist of 2^n horizontal strips and 2^n vertical strips respectively. Clearly the vertical size of each strip in H_n, and the horizontal size of each strip in V_n approaches 0 at least as fast as $R/2^{n-1}$, so

$$H_\infty = \bigcap_{i=0}^{\infty} f^i(\mathcal{S}) \text{ and } V_\infty = \bigcap_{i=0}^{\infty} f^{-i}(\mathcal{S})$$

are unions of horizontal curves and vertical curves respectively, such that $l_h \in H_\infty$ and $l_v \in V_\infty$ intersects in a unique point. Let $\Lambda = V_\infty \cap H_\infty$. We construct a homeomorphism $h : \Lambda \longrightarrow \Sigma_2$ as in [G&H] such that the diagram

$$\begin{array}{ccc} \Lambda & \xrightarrow{f} & \Lambda \\ {\scriptstyle h}\downarrow & & \downarrow{\scriptstyle h} \\ \Sigma_2 & \xrightarrow{\sigma} & \Sigma_2 \end{array}$$

commutes. The periodic points are dense in Σ_2, and Λ is the largest invariant set in $\mathcal{S}$, so $\mathbf{\Omega}(f) = \Lambda$. □

7. Maps with hyperbolic horseshoes

We will show that the topological horseshoe in in the previous section has a hyperbolic structure for a suitable choice of parameters. We will first do some calculations on some certain 2×2-matrices. These calculations will also be useful later when we prove that a qubic family has a hyperbolic non-wandering set homeomorphic to a full shift on three symbols.

Let $M(t,s)$ be the matrix given by

$$M(t,s) = \begin{bmatrix} t & s \\ 1 & 0 \end{bmatrix}$$

and let $N(t,s) = M^{-1}(t,s)$ for $s \neq 0$. Let $k, l > 0$ and let v_k, v_{-k}, w_l and w_{-l} be the four vectors given by $v_k = (1,k)$, $v_{-k} = (1,-k)$, $w_l = (l,1)$ and $w_{-l} = (l,-1)$. v_k and v_{-k} defines a cone by

$$C_{v_k,v_{-k}} = \{v \in \mathbb{R}^2 : v = \gamma(1-\delta)v_k + \gamma\delta v_{-k}, \gamma \in \mathbb{R}, \delta \in [0,1]\},$$

and w_l and w_{-l} defines a cone by

$$C_{w_l,w_{-l}} = \{w \in \mathbb{R}^2 : w = \gamma(1-\delta)w_l + \gamma\delta w_{-l}, \gamma \in \mathbb{R}, \delta \in [0,1]\}.$$

The image of C_{v_k} under $M(t,s)$ is a cone given by $M(t,s)C_{v_k,v_{-k}} = C_{M(t,s)(v_k,v_{-k})}$, and the image of $C_{w_l,w_{-l}}$ under $N(t,s)$ is a cone given by $N(t,s)C_{w_l,w_{-l}} = C_{N(t,s)(w_l,w_{-l})}$. Let $I = [T_1,T_2]$, $T_1 < T_2$, be an interval such that $I \subset \mathbb{R}^-$ or $I \subset \mathbb{R}^+$. For each $t \in I$ $M(t,s)C_{v_k,v_{-k}}$ defines a cone, and we want to find conditions on T_1 and T_2 in terms of s and k such that $M(t,s)C_{v_k,v_{-k}} \subset C_{v_k,v_{-k}}$ for all $t \in I$.
Suppose $I \subset \mathbb{R}^-$ and $s > 0$. Then

$$T_1 - sk \leq t - sk < t + sk \leq T_2 + sk \text{ with } T_1 - sk < 0.$$

Hence we obtain the condition $T_2 + sk \leq -1/k$. If $s < 0$ then

$$T_1 + sk \leq t + sk < t - sk \leq T_2 - sk \text{ with } T_1 + sk < 0,$$

and we obtain the condition $T_2 - sk \leq -1/k$. We conclude that if $I \subset \mathbb{R}^-$ with

$$T_1 < T_2 \leq -\left(\frac{1}{k} + |s|k\right)$$

then $M(t,s)C_{v_k,v_{-k}} \subset C_{v_k,v_{-k}}$ for all $t \in I$. Similar we find that if $I \subset \mathbb{R}^+$ then

$$\frac{1}{k} + |s|k \leq T_1 < T_2$$

implies $M(t,s)C_{v_k,v_{-k}} \subset C_{v_k,v_{-k}}$ for all $t \in I$. We do the same calculations to obtain conditions on T_1 and T_2 in terms of s and l such that $N(t,s)C_{w_l,w_{-l}} \subset C_{w_l,w_{-l}}$ for all $t \in I$.
If $I \subset \mathbb{R}^-$ and $s > 0$, then

$$-s^{-1}(l+T_2) \leq -s^{-1}(l+t) < s^{-1}(l-t) \leq s^{-1}(l-T_1) \text{ with } s^{-1}(l-T_1) > 0,$$

and we obtain the condition $-s^{-1}(l+T_2) \geq 1/l$. If $s < 0$ then

$$s^{-1}(l-T_1) \leq s^{-1}(l-t) < -s^{-1}(l+t) \leq -s^{-1}(l+T_2) \text{ with } s^{-1}(l-T_1) < 0,$$

and we get the condition $-s^{-1}(l+T_2) \leq -1/l$. We conclude that if $I \subset \mathbb{R}^-$ with

$$T_1 < T_2 \leq -\left(l + \frac{|s|}{l}\right)$$

then $N(t,s)C_{w_l,w_{-l}} \subset C_{w_l,w_{-l}}$ for all $t \in I$. Similar we find that if $I \subset \mathbb{R}^+$ then

$$l + \frac{|s|}{l} \leq T_1 < T_2$$

implies $N(t,s)C_{w_l,w_{-l}} \subset C_{w_l,w_{-l}}$ for all $t \in I$.

Lemma 8. *Let $M(t,s)$ and $N(t,s)$ be as above, and let $I_1 = [T_1, T_2] \subset \mathbb{R}^-$, $I_2 = [T_3, T_4] \subset \mathbb{R}^+$, and let $s \neq 0$. Then $M(t,s)C_{v_k,v_{-k}} \subset C_{v_k,v_{-k}}$ for all $t \in I_1 \cup I_2$ if $T_2 \leq -(|s|k + 1/k)$ and $T_3 \geq |s|k + 1/k$, and the distance between I_1 and I_2 has a global minimum for $k = 1/\sqrt{|s|}$. $N(t,s)C_{w_l,w_{-l}} \subset C_{w_l,w_{-l}}$ for all $t \in I_1 \cup I_2$ if $T_2 \leq -(l + |s|/l)$ and $T_3 \geq l + |s|/l$, and the distance between I_1 and I_2 has a global minimum for $l = \sqrt{|s|}$.*

Proof. By the remarks above we only need to show that $d(T_2(k), T_3(k))$ has a global minimum for $k = 1/\sqrt{|s|}$, and that $d(T_2(l), T_3(l))$ has a global minimum for $l = \sqrt{|s|}$. Let $\theta(k) = T_3(k) - T_2(k) = 2(|s|k + 1/k)$ and $\psi(l) = T_3(l) - T_2(l) = 2(l + |s|/l)$. $\theta'(k) = 0$ gives $k = 1/\sqrt{|s|}$ with $\theta''(1/\sqrt{|s|}) > 0$ and $\psi'(l) = 0$ gives $l = \sqrt{|s|}$ with $\psi''(\sqrt{|s|}) > 0$. □

It turns out that the choices of k and l given in lemma 8 are not very useful if we want $M(t,s)$ and $N(t,s)$ to be expansions on $C_{v_k,v_{-k}}$ and $C_{w_l,w_{-l}}$ respectively.

Let $v(\delta) = (1, \delta k)$ and $w(\delta) = (\delta l, 1)$ where $-1 \leq \delta \leq 1$. Then $M(t,s)v(\delta) = (t + \delta k s, 1)$ and $N(t,s)w(\delta) = (1, s^{-1}(\delta l - t))$. By solving a second-degree equation in t we find that $\|M(t,s)v(\delta)\| > \|v(\delta)\|$ for all $\delta \in [-1,1]$ if $t < -(k|s| + k)$ or $t > k|s| + k$, and $\|N(t,s)w(\delta)\| > \|w(\delta)\|$ for all $\delta \in [-1,1]$ if $t < -(l|s| + l)$ or $t > l|s| + l$. Let

$$T_n^M(s,k) = \min\left\{-\left(\frac{1}{k} + k|s|\right), -(k + k|s|)\right\} = \begin{cases} -\left(\frac{1}{k} + k|s|\right), & \text{for } k < 1 \\ -(k + k|s|), & \text{for } k \geq 1 \end{cases}$$

$$T_p^M(s,k) = \max\left\{\left(\frac{1}{k} + k|s|\right), (k + k|s|)\right\} = \begin{cases} \left(\frac{1}{k} + k|s|\right), & \text{for } k < 1 \\ (k + k|s|), & \text{for } k \geq 1 \end{cases}$$

$$T_n^N(s,l) = \min\left\{-\left(\frac{|s|}{l} + l\right), -(l + l|s|)\right\} = \begin{cases} -\left(\frac{|s|}{l} + l\right), & \text{for } l < 1 \\ -(l + l|s|), & \text{for } l \geq 1 \end{cases}$$

$$T_p^N(s,l) = \max\left\{\left(\frac{|s|}{l} + l\right), (l + l|s|)\right\} = \begin{cases} \left(\frac{|s|}{l} + l\right), & \text{for } l < 1 \\ (l + l|s|), & \text{for } l \geq 1 \end{cases}.$$

From lemma 8 and the above we have the following lemma:

Lemma 9. *Let $M(t,s)$ and $N(t,s)$ be as above, and let $I_1 = [T_1, T_2] \subset \mathbb{R}^-$, $I_2 = [T_3, T_4] \subset \mathbb{R}^+$, and let $s \neq 0$. Then $M(t,s)C_{v_k,v_{-k}} \subset C_{v_k,v_{-k}}$ with $\|M(t,s)v\| > \|v\|$, $v \in C_{v_k,v_{-k}}$, for all $t \in I_1 \cup I_2$ if $T_2 \leq T_n^M(s,k)$ and $T_3 \geq T_p^M(s,k)$, and the distance between I_1 and I_2 has a minimum for $k = 1$. The minimum value is $2(1 + |s|)$. $N(t,s)C_{w_l,w_{-l}} \subset C_{w_l,w_{-l}}$ with $\|N(t,s)w\| > \|w\|$, $w \in C_{w_l,w_{-l}}$, for all $t \in I_1 \cup I_2$ if $T_2 \leq T_n^N(s,l)$ and $T_3 \geq T_p^N(s,l)$, and the distance between I_1 and I_2 has a minimum for $l = 1$. The minimum value is $2(1 + |s|)$.*

We will need a better approximation of the non-wanderingset than the approximation given in theorem 2 when $\mathbf{\Omega}(f) \simeq \Sigma_2$. This approximation is given in the following lemma.

Lemma 10. *Let $f \in \mathfrak{f}_{\alpha,\beta}^+$ where $f(x,y) = (\alpha + \beta y - g(x), x)$, and let $\alpha_1(\beta)$ be as in theorem 3. Then for each $\alpha(\beta) > \alpha_1(\beta)$ there exist numbers R_H, R_1 and R_2 with $0 < R_i < R_H$, $i = 1,2$, such that*

$$\mathbf{\Omega}(f) \subset [-R_H, -R_1] \times [-R_H, -R_1] \cup [R_2, R_H] \times [-R_H, -R_1] \cup [R_2, R_H] \times [R_2, R_H] \cup [-R_H, -R_1] \times [R_2, R_H].$$

The number R_H is the positive solution of $h(R) - (1 + |\beta|)R - \alpha = 0$, $h(R) = \min\{g(R), g(-R)\}$, and the numbers $-R_1$ and R_2 are the solutions of $g(R) + (1 + |\beta|)R_H - \alpha = 0$. Furthermore, given any positive number P, there is an $\alpha_P(\beta) > \alpha_1(\beta)$ such that $R_1, R_2 > P$ for all $\alpha(\beta) > \alpha_P(\beta)$.

FIGURE 1.4.
Left: The Hénon-map with $\alpha = 6.5$ and $\beta = 0.7$. **Right:** The Hénon-map with $\alpha = 6.5$ and $\beta = -0.7$. In both cases the area of the square is $4R_H^2$, and the numbers $-R_1$ and R_2 are the second coordinates of the intersection-point with the "inner" horizontal curve and the vertical segment on the right of the square. Since the nonlinear part of the Hénon-map is even we see that $R_1 = R_2$. The sets $f^{-1}(\mathcal{S}(R_H)) \cap \mathcal{S}(R_H) \cap f(\mathcal{S}(R_H))$ where $\mathcal{S}(R_H) = [-R_H, R_H] \times [-R_H, R_H]$ have each four components and are shown in black.

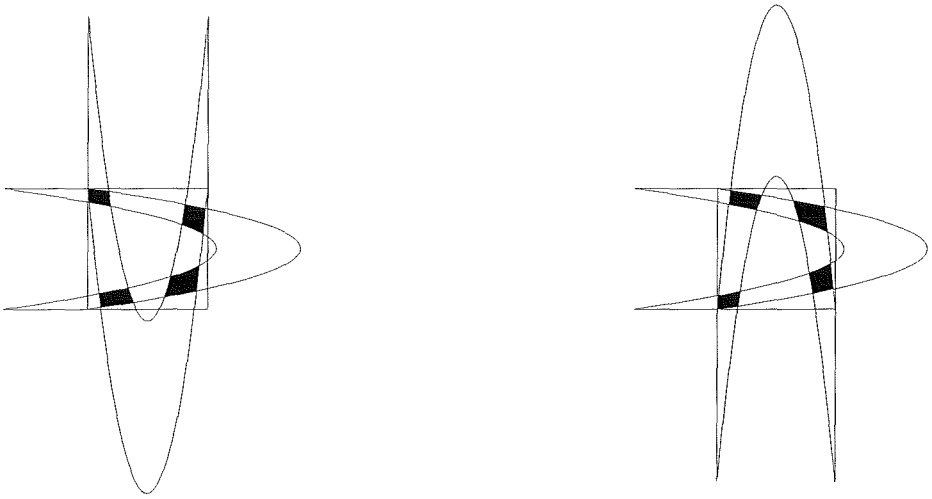

Proof. The existence of the numbers R_1,R_2 and R_H follows from the proof of theorem 3. The approximation of the non-wandering set is simply the approximation used in theorem 2 together with the fact that the images $f(\mathcal{S}(R_H))$ and $f^{-1}(\mathcal{S}(R_H))$ cut completely through $\mathcal{S}(R_H)$ in horizontal and vertical direction respectively.
To complete the proof of the lemma we need to show that $R_i = R_i(\alpha, \beta)$, $i = 1, 2$ are increasing unbounded functions in α. In the following we let $\tilde{R}_1 = -R_1$ and $\tilde{R}_2 = R_2$. We will however refer to $\tilde{R}_1$ and $\tilde{R}_2$ as R_1 and R_2. Consider the defining equations:

$$\begin{aligned} h(R_H(\alpha,\beta) - (1+|\beta|)R_H(\alpha,\beta) - \alpha = 0 \\ g(R_i(\alpha,\beta) + (1+|\beta|)R_H(\alpha,\beta) - \alpha = 0 \end{aligned} \tag{2}$$

From the definition of h we see that h is a continuous piecewise smooth function with the same geometric properties as g. Hence the partial derivatives exist everywhere except at some isolated points. To see that R_H is unbounded we simply note that $h(y) - (1+|b|)y$ is unbounded. To see that R_i is unbounded we note that in the equation $g(x) + 2(1+|\beta|)y - h(y)$ the term $2(1+|\beta|)y - h(y)$ is unbounded. Assume that α is so large that $\frac{\partial h}{\partial x}(R_H(\alpha,\beta)) - 2(1+|\beta|) > 0$. Implicit differentiation of (2) gives

$$\begin{aligned} \frac{\partial R_H}{\partial \alpha}(\alpha,\beta) &= \frac{1}{\dfrac{\partial h}{\partial x}(R_H(\alpha,\beta)) - (1+|\beta|)} \\ \frac{\partial R_i}{\partial \alpha}(\alpha,\beta) &= \frac{1}{\dfrac{\partial g}{\partial x}(R_i(\alpha,\beta))} \left[\frac{\dfrac{\partial h}{\partial x}(R_H(\alpha,\beta)) - 2(1+|\beta|)}{\dfrac{\partial h}{\partial x}(R_H(\alpha,\beta)) - (1+|\beta|)} \right] \end{aligned}$$

It is easy to see that $\frac{\partial R_H}{\partial \alpha}(\alpha,\beta) > 0$, $\frac{\partial R_1}{\partial \alpha}(\alpha,\beta) < 0$ since $R_1 < 0$, and $\frac{\partial R_2}{\partial \alpha}(\alpha,\beta) > 0$ since $R_2 > 0$ which proves the lemma. □

Theorem 4. *Suppose* $f \in \mathfrak{f}^+_{\alpha,\beta}$ *where* $f(x,y) = (\alpha + \beta y - g(x), x)$. *Let* $x_1 = (g')^{-1}(-(1+|\beta|))$, y_1 *be the positive solution of* $h(y) - 2(1+|\beta|)y - g(x_1) = 0$ *and let* $\alpha_{21}(\beta) = g(x_1) + (1+|\beta|)y_1$. *Let* $x_2 = (g')^{-1}(1+|\beta|)$, y_2 *be the positive solution of* $h(y) - 2(1+|\beta|)y - g(x_2) = 0$ *and let* $\alpha_{22}(\beta) = g(x_2) + (1+|\beta|)y_2$. *Let* $\alpha_2(\beta) = \max\{\alpha_{21}, \alpha_{22}\}$. *For every* $\alpha(\beta) > \alpha_2(\beta)$ *there is a homeomorphism* $h_{\alpha(\beta)} : \mathbf{\Omega}(f) \longrightarrow \Sigma_2$ *such that the restriction* $f : \mathbf{\Omega}(f) \longrightarrow \mathbf{\Omega}(f)$ *is topological equivalent to the shiftmap* $\sigma : \Sigma_2 \longrightarrow \Sigma_2$ *and the set* $\mathbf{\Omega}(f)$ *has a hyperbolic structure.*

Proof. By theorem 3 the topological equivalence to the shiftmap on the non-wandering set is clear since $\alpha_2(\beta) > \alpha_1(\beta)$. We only need to show that the non-wandering set has a hyperbolic structure.

Let $f \in \mathfrak{f}^+_{\alpha,\beta}$ where $f(x,y) = (\alpha + \beta y - g(x), x)$. Then

$$Df_{\alpha,\beta}(x,y) = \begin{bmatrix} -g'(x) & \beta \\ 1 & 0 \end{bmatrix} \quad \text{and} \quad Df^{-1}_{\alpha,\beta}(x,y) = \begin{bmatrix} 0 & 1 \\ \beta^{-1} & \beta^{-1}g'(y) \end{bmatrix}.$$

Let $-g(x) = t$ and $\beta = s$ in $Df_{\alpha,\beta}(x,y)$. We obtain the matrix $M(t,s)$. Let $k = 1$. Lemma 9 implies that $M(t,s)$ is an expansion on the cone $C_{v_1,v_{-1}}$ if $t > 1 + |s|$ or $t < -(1+|s|)$. Hence $Df_{\alpha,\beta}(x,y)$ is an expansion on the cone $C_{v_1,v_{-1}}$ if $x < (g')^{-1}(-(1+|\beta|))$ or $x > (g')^{-1}(1+|\beta|)$. Similarly, with $g'(y) = t$ and $\beta = s$ in $Df^{-1}_{\alpha,\beta}(x,y)$ we obtain $N(t,s)$, and find that $Df^{-1}_{\alpha,\beta}(x,y)$ is an expansion on the cone $C_{w_1,w_{-1}}$ if $y < (g')^{-1}(-(1+|\beta|))$ or $y > (g')^{-1}(1+|\beta|)$.

Let $P = \min\{-(g')^{-1}(-(1+|\beta|)), (g')^{-1}(1+|\beta|)\}$. Then by lemma 9, lemma 10 and the remarks above $Df_{\alpha,\beta}(x,y)$ maps $C_{v_1,v_{-1}}$ to $C_{v_1,v_{-1}}$ and is an expansion on the cone, and $Df^{-1}_{\alpha,\beta}(x,y)$ maps $C_{w_1,w_{-1}}$ to $C_{w_1,w_{-1}}$ and is an expansion one the cone in each tangent space over $\mathbf{\Omega}(f)$ for $\alpha(\beta) > \alpha_P(\beta)$.

In the theorem from [New] stated in section 1 we use a constant splitting of the tangent space such that the matrix of Df relative to this splitting is the usual Jacobi matrix, and let $\epsilon(p) = 1$. Then the sectors $S_{\epsilon(p)}$ and $S'_{\epsilon(p)}$ are independent on p and are the cones $C_{v_1,v_{-1}}$ and $C_{w_1,w_{-1}}$ respectively. Hence the conditions in the theorem [New] is satisfied, and $\mathbf{\Omega}(f)$ is hyperbolic for $\alpha(\beta) > \alpha_P(\beta)$.

The estimate on P is obtained by lemma 9, lemma 10 and the proof of theorem 3. □

Remark. The parameter value $\alpha_2(\beta)$ in theorem 4 is larger than the parameter value $\tilde{\alpha}_2(\beta)$ where the tangent bundle over topological horseshoe gets a hyperbolic structure. There are several reasons for this; The approximation of the non-wandering set given in lemma 10 is not the best possible. Another factor is the choice of domain to construct the horseshoe. We have used a square for technical reasons, but other domains may give better approximations, but the calculations to prove that the non-wandering set is contained in its interior, and the calculations to obtain conditions for a horseshoe may be difficult. We give below a modified version of lemma 10 for $f \in \mathfrak{f}^+_{\alpha,\beta}$, given by $(x,y) \mapsto (\alpha + \beta y - g(x), x)$, where g is even, and apply this to the Hénon family in the example below. It will then be clear how to extend this argument to modify lemma 10 to an arbitrarily f in $\mathfrak{f}^+_{\alpha,\beta}$. However, this will not be done here.

If $f \in \mathfrak{f}^+_{\alpha,\beta}$ is even then the image of the square containing the non-wandering set looks like the images in figure 1.4. We approximate the non-wandering set by four rectangles as in lemma 10, but instead of using the intersection of the boundary with its images by f and f^{-1}, we use the intersections of just the images. For an even g the nearest intersection point to the y-axis will control the approximation. In figure 1.4 this is the intersection at the lower right corner of the lower left black set for $\beta > 0$, and the upper right corner of the upper black set for $\beta < 0$. It is easily seen that the relevant points satisfy the equations

$$\begin{aligned} g(x) - \beta y + R_H - \alpha &= 0 \\ g(y) + x - |\beta| R_H - \alpha &= 0. \end{aligned} \tag{3}$$

The relevant solution is the point with negative x-coordinate, and smallest norm of this coordinate. We denote this solution by $(-\tilde{R}_1, \tilde{y})$, and obtain the following approximation of $\mathbf{\Omega}(f)$:

$$\mathbf{\Omega}(f) \subset [-R_H, -\tilde{R}_1]\times[-R_H, -\tilde{R}_1] \cup [\tilde{R}_1, R_H]\times[-R_H, -\tilde{R}_1] \cup [\tilde{R}_1, R_H]\times[\tilde{R}_1, R_H] \cup [-R_H, -\tilde{R}_1]\times[\tilde{R}_1, R_H].$$

Now using the assumption that g is even we find that $\mathbf{\Omega}(f)$ is hyperbolic if $|x| > (g')^{-1}(1+|\beta|)$ for all $(x,y) \in \mathbf{\Omega}(f)$. Eliminating α from (3) we obtain $g(x) - \beta y + R_H - g(y) - x + |\beta| R_H = 0$. As before R_H is the positive solution of $g(R) - 2(1+|\beta|)R = 0$. From the hyperbolicity condition we get $R_1 = (g')^{-1}(1+|\beta|)$. Let $\tilde{y}$ be the smallest solution of $g(y) + \beta y - R_1 - g(R_1) - (1+|\beta|)R_H = 0$ if $\beta > 0$ and $\tilde{y}$ be the largest solution of the equation if $\beta < 0$. The new estimate $\alpha_2^1(\beta)$ is given by

$$\alpha_2^1(\beta) = g(R_1) - \beta\tilde{y} + R_H,$$

and by the construction we see that $\tilde{\alpha}_2(\beta) \le \alpha_2^1(\beta) \le \alpha_2^1(\beta)$.

Example. In this example we apply the proof of theorem 3 and theorem 4 to given families $(x,y) \mapsto (\alpha + \beta y - g(x), x)$. Similar results for the Hénon family can be found in [Dev], but not the estimates on $\alpha_2^1(\beta)$.

In the Hénon family $g(x) = h(x) = x^2$ and $(g')^{-1}(x) = x/2$. With the notation in theorem 3 we have $r(R) = R^2 - (1+|\beta|)R$ and $l(R) = (1+|\beta|)R$. Then the positive solution of $r(R) = l(R)$ is $R_H = 2(1+|\beta|)$, and by theorem 3 $\alpha_1(\beta) = l(R_H) = 2(1+|\beta|)^2$.

In theorem 4 we observe that for a symmetric g it is sufficient to compute x_2 and y_2. We find that $x_2 = (g')^{-1}(1+|\beta|) = (1+|\beta|)/2$. The positive solution of

$$h(y) - 2(1+|\beta|)y - g(x_2) = y^2 - 2(1+|\beta|)y - \frac{(1+|\beta|)^2}{4} = 0$$

is given by

$$y_2 = \frac{2(1+|\beta|) + \sqrt{4(1+|\beta|)^2 + (1+|\beta|)^2}}{2} = \left(\frac{2+\sqrt{5}}{2}\right)(1+|\beta|)$$

so

$$\alpha_2(\beta) = g(x_2) + (1+|\beta|)y_2 = \frac{(1+|\beta|)^2}{4} + \left(\frac{2+\sqrt{5}}{2}\right)(1+|\beta|)^2 = \left(\frac{5+2\sqrt{5}}{4}\right)(1+|\beta|)^2.$$

Applying the method to find $\alpha_2^1(\beta)$ in the remark above to the Hénon family we find $R_H = 2(1+|\beta|)$, $R_1 = (1+|\beta|)/2$ and

$$\tilde{y} = \begin{cases} -\frac{1}{2}\left(\beta + \sqrt{\beta^2 + 2(1+|\beta|) + 9(1+|\beta|)^2}\right) & \text{if } \beta > 0 \\ -\frac{1}{2}\left(\beta - \sqrt{\beta^2 + 2(1+|\beta|) + 9(1+|\beta|)^2}\right) & \text{if } \beta < 0 \end{cases}$$

so

$$\begin{aligned} \alpha_2^1(\beta) &= \frac{1}{4}\left(8(1+|\beta|) + (1+|\beta|)^2 + 2|\beta|\left(|\beta| + \sqrt{\beta^2 + 2(1+|\beta|) + 9(1+|\beta|)^2}\right)\right) \\ &= \frac{1}{4}\left(9 + 10|\beta| + 3\beta^2 + 2|\beta|\sqrt{10(1+|\beta|^2 + 1}\right). \end{aligned}$$

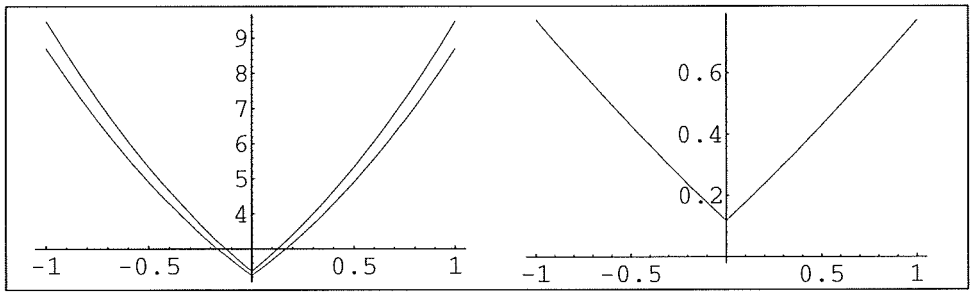

FIGURE 1.5.
Left: The curves $\alpha = \alpha_2(\beta)$ and $\alpha = \alpha_2^1(\beta)$ for the Hénon family. **Right:** The difference between $\alpha = \alpha_2(\beta)$ and $\alpha = \alpha_2^1(\beta)$. The plot shows $\alpha_2(\beta) - \alpha_2^1(\beta)$.

If we apply the proof of theorem 3 and theorem 4 to a hyperbolic cosine family $(x,y) \mapsto (\alpha + \beta y - (\cosh x - 1), x)$, to a logarithmic family $(x,y) \mapsto (\alpha + \beta y - ((1+|x|)\ln(1+|x|) - |x|), x)$, to the Hénon family with an oscillating term added and to a family with a non-symmetric non-linear part $(x,y) \mapsto (\alpha + \beta y - s(x), x)$ where

$$s(x) = \begin{cases} \cosh x - 1 & \text{for } x < 0 \\ \dfrac{x^2}{2} & \text{for } x \geq 0 \end{cases}$$

we obtain numerically by a simple *Mathematica*-program the curves $\alpha_1(\beta)$ and $\alpha_2(\beta)$ plotted in figure 1.6.

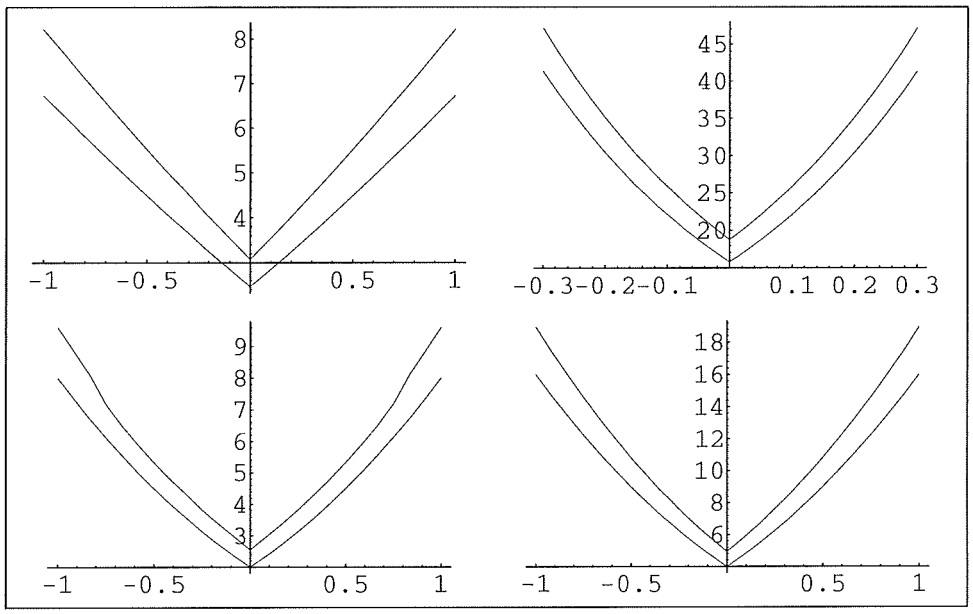

FIGURE 1.6.

In all four plots α_i, $i = 1, 2$, is plotted as a function of β. The lower curve, $\alpha_1(\beta)$, is a bound for where the family has a non-wandering set conjugate to a 2-shift, and the higher curve $\alpha_2(\beta)$ is a bound for where the non-wandering set has a hyperbolic structure.

Upper left: The curves hyperbolic cosine family. **Upper right:** The logarithmic family **Lower left:** The Hénon family with an oscillating term. **Lower right:** A family with a non-symmetric non-linear part.

8. PHASE DIAGRAMS AND COMPUTER EXPERIMENTS

In this section we describe, and give the result of some numerical experiments with $\mathrm{f}^{+}_{\alpha,\beta}$-type systems, and with a cubic system described in section 9. We will consider the following systems:

List of families.

Family 1) $(x,y) \mapsto (\alpha + \beta y - x^2, x)$
Family 2) $(x,y) \mapsto (\alpha + \beta y - (\cosh x - 1), x)$
Family 3) $(x,y) \mapsto (\alpha + \beta y - ((1+|x|)\ln(1+|x|) - |x|), x)$
Family 4) $(x,y) \mapsto (\alpha + \beta y - (x^2 + \dfrac{\cos(14x) - 1}{112}, x)$
Family 5) $(x,y) \mapsto (\alpha + \beta y - s(x), x)$
Family 6) $(x,y) \mapsto (\beta y + x^3 - \alpha^2 x, x)$

where

$$s(x) = \begin{cases} \cosh x - 1 & \text{for } x < 0 \\ \dfrac{x^2}{2} & \text{for } x \geq 0. \end{cases}$$

The families above have been chosen so they display typical behavior we might find in the class $\mathfrak{f}^+_{\alpha,\beta}$. Family 1 is the Hénon-family, and the non-linear part is a second-degree polynomial. This family has been included as a reference, since a lot of numerical experiments has been done with this family. Family 2 has a exponential nonlinear part. The non-linear part of family 3 is growing slower than any map of the form $x \mapsto x^{1+\epsilon}$ for any $\epsilon > 0$. In family 4 we have added a small oscillating term to the Hénon family. Family 5 is not even in x and is not very smooth. The family is C^1, but not C^2.

The first sequence of experiments is concerned with the existence of numerical strange attractors in the systems. The second sequence of experiments is concerned with both-ways pitch-forks in the bifurcation diagram of the systems. We will first give a short description of the experiments and a list of the content of the figures. At the end we sum up the observations and give some remarks.

Strange attractors. By a strange attractor we will mean the following (These definitions is taken from [G&H]):

A closed f-invariant set Λ is called indecomposable if for every pair of points x, y in Λ and $\epsilon > 0$, there are $x = x_0, x_1, \ldots, x_{n-1}, x_n = y$ and $m_1, \ldots, m_n \geq 1$ such that the distance from $f^{m_i}(x_{i-1})$ to x_i is smaller than ϵ.

An attractor is an indecomposable closed f-invariant set Λ with the property that, given $\epsilon > 0$, there is a set U of positive Lebesgue measure in the ϵ-neighborhood of Λ such that $x \in U$ implies that the ω-limit set of x is contained in Λ, and the forward orbit of x is contained in U. We shall call an attractor strange if it contains a transversal homoclinic orbit.

Let M denote a computer with a given floating-point accuracy ϵ_M and N_M integer range.

By a numerical strange attractor on M for a system in $\mathbb{R}^2$ we will mean the following:

(1) Let $N < N_M$ be any positive integer less than the computer integer range. There exists an open bounded set W independent of N, such that if $x_0 \in W$ then $f^n(x_0) \in W$ for $n \in \{1, \ldots, N\}$. The set $A_N = \cap_{j=0}^{N} f^j(W)$ is called a numerical attracting set.

(2) Let $\epsilon > \epsilon_M$ and let $B_\epsilon(x)$ denote the ϵ-ball of x. Let $x_0 \in A_N$ with $N < N_E/2$. Then for almost all $y_0 \in W$ the positive finite orbit $\{y_i\}_{i=0}^{N_E}$ where $y_{i+1} = f(y_i)$, intersects $B_\epsilon(x_p)$.

(3) There exists a periodic point p of saddle-type in A_N for any $N < N_M$.

Property (1) states that for a set of initial values the orbits stay bounded. Here we see that property (2) replaces the indecomposable condition above, and condition (3) together with (2) replace the homoclinic orbit condition.

Experiment 1: Existence of an attracting set. We plot the orbits of several hundred initial values inside some bounded set, and observe if we have stable periodic orbits or something else.

Experiment 2: The indecomposable condition. We observe the attracting set for a single orbit, and compare with the results of experiment 1.

Experiment 3: The structure of the attractor. We magnify a part of the phase space near a fixed point of saddle-type.

Experiment 4: Domain of attraction. We find initial values such that the forward orbit is bounded.

Experiment 5: Liapunov numbers. We compute the largest Liapunov number for parameter values close to the parameter values for the attractor.

Experiment 6: Both-ways pitch-fork bifurcations. We investigate the bifurcation diagram of some systems looking for both-ways pitch-fork bifurcations.

Bifurcation diagrams. In [K&K&Y] it is proven that in any one-parameter family $\{f_\lambda\}$ of dissipative plane C^3-diffeomorphisms with a non-degenerate homoclinic tangency parameter value $\lambda = \lambda_0$, then there exist both orbit creating and orbit annihilating parameter values arbitrarly close to λ_0. The proof of this uses the fact that for λ_1 arbitrarly close to $\lambda = \lambda_0$ there exits a hyperbolic basic set $\Lambda(f_{\lambda_1})$ whose product

of stable and unstable thichness is greater than one, and the system f_{λ_1} has a periodic point q contained in $\Lambda(f_{\lambda_1})$ with a non-degenerate homoclinic tangency.

The anti-monotone behavior arising from the above theorem could be hard to detect numerically because the dynamics involved with a homoclinic tangency (or a transversal homoclinic point) is extremly complicated, and the domain of attraction of periodic points is small. The period of the point q may also be large. Hence we should expect to see chaotic behavior numerically near homoclinic tangency parameter values, and not be able to detect periodic orbits.

It is our belief that the computed example for the Hénon system does not illustrate the theorem in the paper. We belive that we see a stable periodic orbit bifurcating in a period-doubling bifurcation at $\alpha = \alpha'$ and becomes unstable. However, for some $\alpha = \alpha''$ the same periodic orbit becomes stable again, and the result is a sequence, finite or infinite, of both-ways pitch-forks. This phenomenon is discussed in a comming paper.

The existence of infinite sequences of pitch-forks followed by a reversed infinite sequence of pitch-forks seems to be common in the systems considered here. We have given examples of such bifurcation sequences for each system defined above.

Figure 1 – 6 shows the attractor where the orbit of many initial values are plotted in the same picture.
Figure 1: The Hénon attractor. A strange attractor for $(x, y) \mapsto (\alpha + \beta y - x^2, x)$ with $\alpha = 1.4$ and $\beta = 0.3$. We have used 200 different initial points, each iterated 20 times and then plotted the 1000 next.

Figure 2: A Hénon like attractor. A strange attractor for $(x, y) \mapsto (\alpha + \beta y - (\cosh x - 1), x)$ with $\alpha = 1.56$ and $\beta = 0.4$. We have used 200 different initial points, each iterated 20 times and then plotted the 1000 next.

Figure 3: A Hénon like attractor. A strange attractor for $(x, y) \mapsto (\alpha + \beta y - ((1 + |x|)\ln(1 + |x|) - |x|), x)$ with $\alpha = 10.4$ and $\beta = 0.3$. We have used 200 different initial points, each iterated 20 times and then plotted the 1000 next.

Figure 4: A Hénon like attractor. A strange attractor for $(x, y) \mapsto (\alpha + \beta y - (x^2 + \frac{\cos(14x) - 1}{112}, x)$ with $\alpha = 1.41$ and $\beta = 0.3$. We have used 200 different initial points, each iterated 20 times and then plotted the 1000 next.

Figure 5: A Hénon like attractor. A strange attractor for $(x, y) \mapsto (\alpha + \beta y - s(x), x)$ with $\alpha = 2.1$ and $\beta = 0.4$. Here

$$s(x) = \begin{cases} \cosh x - 1 & \text{for } x < 0 \\ \dfrac{x^2}{2} & \text{for } x \geq 0. \end{cases}$$

We have used 200 different initial points, each iterated 20 times and then plotted the 1000 next.

Figure 6: A Hénon like attractor. A strange attractor for $(x, y) \mapsto (\beta y + x^3 - \alpha^2 x, x)$ with $\alpha = 1.55$ and $\beta = 0.3$. We have used 200 different initial points, each iterated 20 times and then plotted the 1000 next.

Figures 7 – 12 show the attractor where the orbit of a single initial value is plotted. The figures appear to be the same as in figures 1 – 6.
Figure 7: The Hénon attractor. A strange attractor for $(x, y) \mapsto (\alpha + \beta y - x^2, x)$ with $\alpha = 1.4$ and $\beta = 0.3$. We have used a single initial point iterated 100 times and then plotted the 200000 next.

Figure 8: A Hénon like attractor. A strange attractor for $(x, y) \mapsto (\alpha + \beta y - (\cosh x - 1), x)$ with $\alpha = 1.56$ and $\beta = 0.4$. We have used a single initial initial point iterated 100 times and then plotted the 200000 next.

Figure 9: A Hénon like attractor. A strange attractor for $(x, y) \mapsto (\alpha + \beta y - ((1 + |x|)\ln(1 + |x|) - |x|), x)$

with $\alpha = 10.4$ and $\beta = 0.3$. We have used a single initial initial point iterated 100 times and then plotted the 200000 next.

Figure 10: A Hénon like attractor. A strange attractor for $(x, y) \mapsto (\alpha + \beta y - (x^2 + \frac{\cos(14x) - 1}{112}, x)$ with $\alpha = 1.41$ and $\beta = 0.3$. We have used a single initial initial point iterated 100 times and then plotted the 200000 next.

Figure 11: A Hénon like attractor. A strange attractor for $(x, y) \mapsto (\alpha + \beta y - s(x), x)$ with $\alpha = 2.1$ and $\beta = 0.4$. Here

$$s(x) = \begin{cases} \cosh x - 1 & \text{for } x < 0 \\ \dfrac{x^2}{2} & \text{for } x \geq 0. \end{cases}$$

We have used a single initial initial point iterated 100 times and then plotted the 200000 next.

Figure 12: A Hénon like attractor. A strange attractor for $(x, y) \mapsto (\beta y + x^3 - \alpha^2 x, x)$ with $\alpha = 1.55$ and $\beta = 0.3$. We have used a single initial initial point then plotted the 200000 next.

In figures 13 – 24 we show magnifications of the orbit structure near a fixed point of sadle-type in the attractor. We observe in each case the same structure of orbits as in the Hénon attractor.
Figure 13: A magnification of the Hénon attractor near the fixed point at $(0.883896, 0.883896)$. The attractor appears locally to be an interval crossed with a Cantor set. We have used 500 initial values each iterated 100 times, and then plotted the part of the next 2000 points on the orbit inside the current window.

Figure 14: A magnification of the last figure near the fixed point. We have used 1000 initial values each iterated 100 times, and then plotted the part of the next 4000 points on the orbit inside the current window.

Figure 15: A magnification of a Hénon like attractor for the system $(x, y) \mapsto (\alpha + \beta y - (\cosh x - 1), x)$ with $\alpha = 1.56$ and $\beta = 0.4$ near the fixed point at $(1.21383, 1.21383)$. The attractor appears to have the same structure as the Hénon attractor. We have used 500 initial values each iterated 100 times, and then plotted the part of the next 2000 points on the orbit inside the current window.

Figure 16: A magnification of the last figure near the fixed point. We have used 1000 initial values each iterated 100 times, and then plotted the part of the next 4000 points on the orbit inside the current window.

Figure 17: A magnification of a Hénon like attractor for the system $(x, y) \mapsto (\alpha + \beta y - ((1 + |x|) \ln(1 + |x|) - |x|), x)$ with $\alpha = 10.4$ and $\beta = 0.3$ near the fixed point at $(5.45456, 5.45456)$. The attractor appears to have the same structure as the Hénon attractor. We have used 500 initial values each iterated 100 times, and then plotted the part of the next 2000 points on the orbit inside the current window.

Figure 18: A magnification of the last figure near the fixed point. We have used 1000 initial values each iterated 100 times, and then plotted the part of the next 4000 points on the orbit inside the current window.

Figure 19: A magnification of a Hénon like attractor for the system $(x, y) \mapsto (\alpha + \beta y - (x^2 + \frac{\cos(14x) - 1}{112}, x)$ with $\alpha = 1.41$ and $\beta = 0.3$ near the fixed point at $(0.887975, 0.887975)$. The attractor appears to have the same structure as the Hénon attractor. We have used 500 initial values each iterated 100 times, and then plotted the part of the next 2000 points on the orbit inside the current window.

Figure 20: A magnification of the last figure near the fixed point. We have used 1000 initial values

each iterated 100 times, and then plotted the part of the next 4000 points on the orbit inside the current window.

Figure 21: A magnification of a Hénon like attractor for the system $(x, y) \mapsto (\alpha + \beta y - s(x), x)$ with $\alpha = 2.1$ and $\beta = 0.4$ near the fixed point at $(1.53542, 1.53542)$. The attractor appears to have the same structure as the Hénon attractor. We have used 500 initial values each iterated 100 times, and then plotted the part of the next 2000 points on the orbit inside the current window.

Figure 22: A magnification of the last figure near the fixed point. We have used 1000 initial values each iterated 100 times, and then plotted the part of the next 4000 points on the orbit inside the current window.

Figure 23: A magnification of a Hénon like attractor for the system $(x, y) \mapsto (\beta y + x^3 - \alpha^2 x, x)$ with $\alpha = 1.55$ and $\beta = 0.3$ near the fixed point at $(0, 0)$. The attractor appears to have the same structure as the Hénon attractor. We have used 500 initial values each iterated 100 times, and then plotted the part of the next 2000 points on the orbit inside the current window.

Figure 24: A magnification of the last figure near the fixed point. We have used 1000 initial values each iterated 100 times, and then plotted the part of the next 4000 points on the orbit inside the current window.

In figures 25 – 30 we have plotted initial values with non-bounded orbits in black. Initialvalues with bounded orbits are shown in white. The attractor is shown in the middle of the figures.
Figure 25: The system $(x, y) \mapsto (\alpha + \beta y - x^2, x)$, $\alpha = 1.4$ and $\beta = 0.3$, with initial values giving non-bounded orbits in black.

Figure 26: The system $(x, y) \mapsto (\alpha + \beta y - (\cosh x - 1), x)$, $\alpha = 1.56$ and $\beta = 0.4$, with initial values giving non-bounded orbits in black.

Figure 27: The system $(x, y) \mapsto (\alpha + \beta y - ((1 + |x|)\ln(1 + |x|) - |x|), x)$, $\alpha = 10.4$ and $\beta = 0.3$, with initial values giving non-bounded orbits in black.

Figure 28: The system $(x, y) \mapsto (\alpha + \beta y - (x^2 + \frac{\cos(14x) - 1}{112}, x)$, $\alpha = 1.41$ and $\beta = 0.3$, with initial values giving non-bounded orbits in black.

Figure 29: The system $(x, y) \mapsto (\alpha + \beta y - s(x), x)$, $\alpha = 2.1$ and $\beta = 0.4$, with initial values giving non-bounded orbits in black.

Figure 30: The system $(x, y) \mapsto (\beta y + x^3 - \alpha^2 x, x)$, $\alpha = 1.55$ and $\beta = 0.3$, with initial values giving non-bounded orbits in black.

Figures 31 – 36 show the largest Liapunov number of an attracting set for parameter values near the attractors considered above. We variy α and keep β fixed. In each case we have chosen a tangent vector at random, iterated 400 times while keeping track of the direction of the tangent, and then used the 1000 next points on the orbit to estimate the Liapunov exponent. In each case the second axis has scale 0 to 1.
Figure 31: The largest Liapunov number for the system $(x, y) \mapsto (\alpha + \beta y - x^2, x)$ when α is varied from 1.39 to 1.41 and β fixed at 0.3.

Figure 32: The largest Liapunov number for the system $(x, y) \mapsto (\alpha + \beta y - (\cosh x - 1), x)$ when α is varied from 1.55 to 1.57 and β fixed at 0.4.

Figure 33: The largest Liapunov number for the system $(x,y) \mapsto (\alpha + \beta y - ((1+|x|)\ln(1+|x|) - |x|), x)$ when α is varied from 10.3 to 10.4 and β fixed at 0.3.

Figure 34: The largest Liapunov number for the system $(x,y) \mapsto (\alpha + \beta y - (x^2 + \frac{\cos(14x)-1}{112}, x)$ when α is varied from 1.4 to 1.42 and β fixed at 0.3.

Figure 35: The largest Liapunov number for the system $(x,y) \mapsto (\alpha + \beta y - s(x), x)$ when α is varied from 2.09 to 2.11 and β fixed at 0.4.

Figure 36: The largest Liapunov number for the system $(x,y) \mapsto (\beta y + x^3 - \alpha^2 x, x)$ when α is varied from 1.54 to 1.56 and β fixed at 0.3.

Figures 37 – 42 show the largest Liapunov number of an attracting set for parameter values near the attractors considered above. We variy β and keep α fixed. In each case we have chosen a tangent vector at random, iterated 400 times while keeping track of the direction of the tangent, and then used the 1000 next points on the orbit to estimate the Liapunov exponent. In each case the second axis has scale 0 to 1.
Figure 37: The largest Liapunov number for the system $(x,y) \mapsto (\alpha + \beta y - x^2, x)$ when β is varied from 0.299 to 0.301 and α fixed at 1.4.

Figure 38: The largest Liapunov number for the system $(x,y) \mapsto (\alpha + \beta y - (\cosh x - 1), x)$ when β is varied from 0.399 to 0.401 and α fixed at 1.56.

Figure 39: The largest Liapunov number for the system $(x,y) \mapsto (\alpha + \beta y - ((1+|x|)\ln(1+|x|) - |x|), x)$ when β is varied from 0.295 to 0.305 and α fixed at 10.4.

Figure 40: The largest Liapunov number for the system $(x,y) \mapsto (\alpha + \beta y - (x^2 + \frac{\cos(14x)-1}{112}, x)$ when β is varied from 0.299 to 0.301 and α fixed at 1.41.

Figure 41: The largest Liapunov number for the system $(x,y) \mapsto (\alpha + \beta y - s(x), x)$ when β is varied from 0.399 to 0.401 and α fixed at 2.1.

Figure 42: The largest Liapunov number for the system $(x,y) \mapsto (\beta y + x^3 - \alpha^2 x, x)$ when β is varied from 0.299 to 0.301 and α fixed at 1.55.

Figures 43 – 48 show examples of infinite sequences of both-ways pitch-fork bifurcations. In each case we consider a one-parameter family of diffeomorphisms with a constant Jacobi determinant. By the term base period in the figures below we mean the period of the stable orbit at the first period-doubling bifurcation. In each figure we have the parameter axis along the horizontal axis and the x-component of the phase variable along the vertical axis.
Figure 43: Both-ways pitch-forks in $(x,y) \mapsto (\alpha + \beta y - x^2, x)$ with $(\alpha, x) \in [1.52, 1.55] \times [-1.1538, -0.908]$ and $\beta = 0.217$. The base period is 6. This is not the example from [K&K&Y].

Figure 44: Both-ways pitch-forks in $(x,y) \mapsto (\alpha + \beta y - (\cosh x - 1), x)$ with $(\alpha, x) \in [2.0954, 2.10813] \times [1.81121, 1.86159]$ and $\beta = 0.15$. The base period is 6.

Figure 45: Both-ways pitch-forks in $(x,y) \mapsto (\alpha + \beta y - ((1+|x|)\ln(1+|x|) - |x|), x)$ with $(\alpha, x) \in [8.21, 8.57] \times [-1.228, -0.775]$ and $\beta = 0.201$. The base period is 10.

Figure 46: Both-ways pitch-forks in $(x,y) \mapsto (\alpha + \beta y - (x^2 + \frac{\cos(14x)-1}{112}, x)$ with $(\alpha, x) \in [1.599, 1.603] \times [-1.394, -1.3548]$ and $\beta = 0.17011$. The base period is 18.

Figure 47: Both-ways pitch-forks in $(x, y) \mapsto (\alpha + \beta y - s(x), x)$ with $(\alpha, x) \in [2.0558, 2.0563] \times [1.123, 1.13]$ and $\beta = 0.3499$. The base period is 19.

Figure 48: Both-ways pitch-forks in $(x, y) \mapsto (\beta y + x^3 - \alpha^2 x, x)$ with $(\alpha, x) \in [1.485, 1.493] \times [-1.18, -0.62]$ and $\beta = 0.1298$. The base period is 10. We see two branches of the 10-periodic orbit.

Conclutions. We conclude from the experiments above that the attracting sets in figures 1 – 6 are numerical strange attractors. The Hénon attractor is by most authors reconized as a strange attractor in the sense of [G&H]. It seems that Hénon like attractors occurs in most systems bifurcating from a finite non-wandering set to a full shift. These numerical strange attractors seems to be in some sense stable (fig. 31 – 42) since the largest Liapunov number seems to be positive in some neighborhood of the parameter value of the attractor. It follows from the computation in section 7 that the attracting sets are non-hyperbolic.

We also conclude that non-monotone behavior on a larger scale than predicted in [K&K&Y] is common in one-parameter families of plane dissipative diffeomorphisms with constant Jacobi determinant. This phenomenon should be further studied.

The numerical experiments was performed on a Macintosh IIsi using the programs `ps-dyn` and `bif-tool` written by Tore M. Jonassen in Think C. The program `ps-dyn` produces POSTSCRIPT output of phase-diagrams, bigurcation diagrams and Liapunov-exponent diagrams for discrete dynamical systems. The program `bif-tool` is a screen-zoom tool to investigate bifurcation diagrams.

$\alpha = 1.400000$, $\beta = 0.300000$ ***Figure 1***
Map = 1, P = 200, N = 1000, I = 20
$(x,y) \in [-2.000000,2.000000] \times [-2.000000,2.000000]$

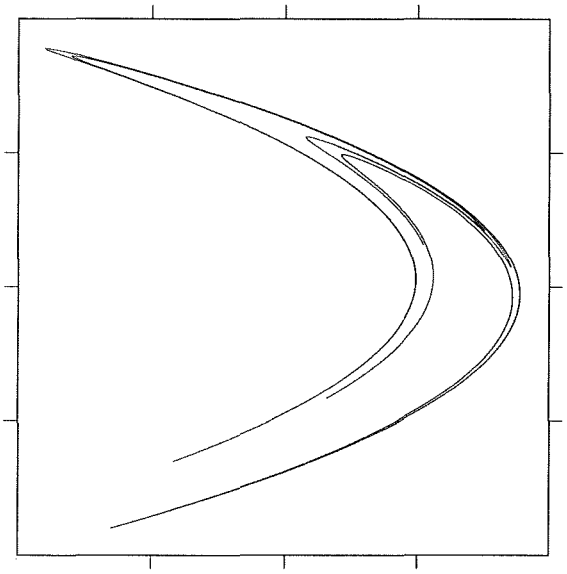

$\alpha = 1.560000$, $\beta = 0.400000$ ***Figure 2***
Map = 2, P = 200, N = 1000, I = 20
$(x,y) \in [-2.500000,2.500000] \times [-2.500000,2.500000]$

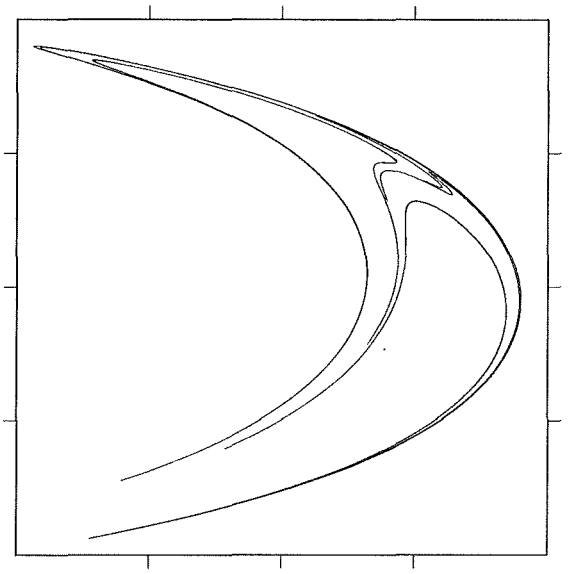

$\alpha = 10.400000$, $\beta = 0.300000$ ***Figure 3***
Map = 3, P = 200, N = 1000, I = 20
$(x,y) \in [-14.000000,14.000000] \times [-14.000000,14.000000]$

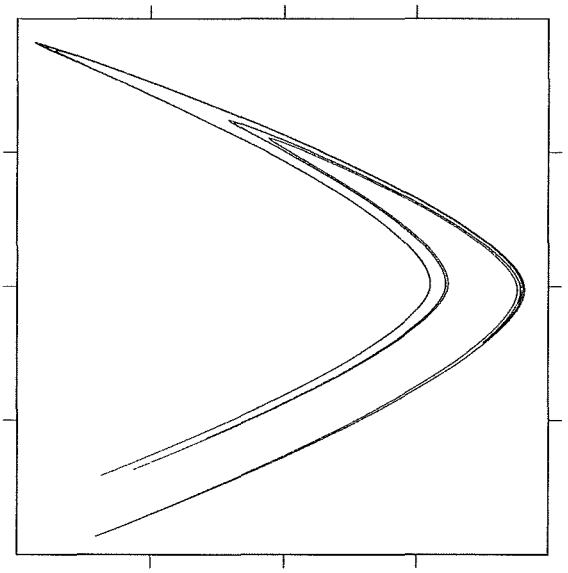

$\alpha = 1.410000$, $\beta = 0.300000$ ***Figure 4***
Map = 4, P = 200, N = 1000, I = 20
$(x,y) \in [-2.000000,2.000000] \times [-2.000000,2.000000]$

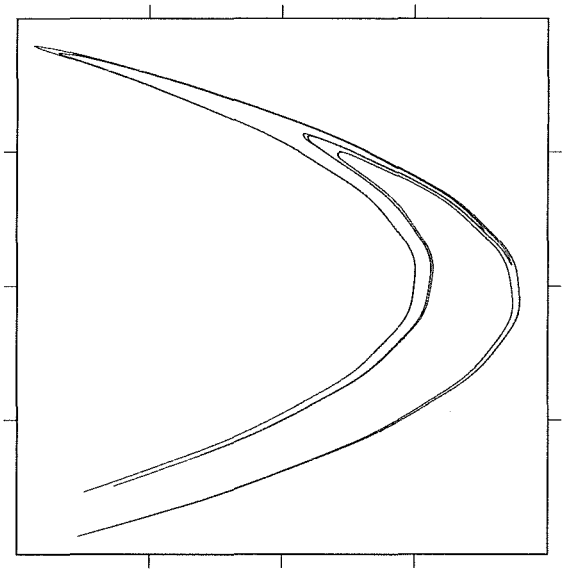

$\alpha = 2.100000$, $\beta = 0.400000$ ***Figure 5***
Map = 5, P = 200, N = 1000, I = 20
$(x,y) \in [-3.250000,3.250000] \times [-3.250000,3.250000]$

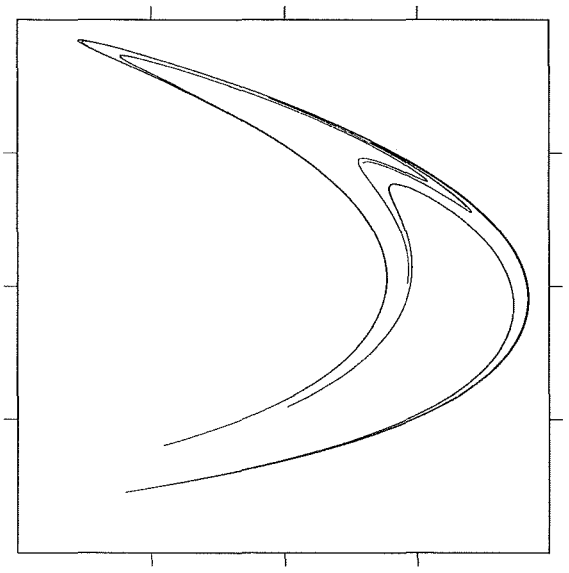

$\alpha = 1.550000$, $\beta = 0.300000$ ***Figure 6***
Map = 6, P = 200, N = 1000, I = 20
$(x,y) \in [-2.000000,2.000000] \times [-2.000000,2.000000]$

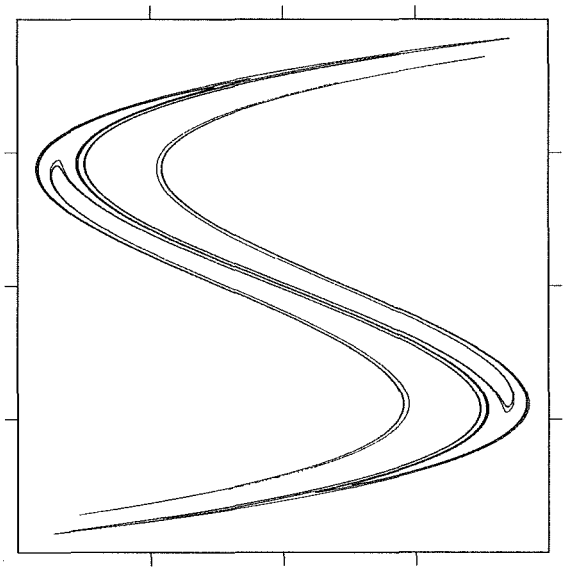

$\alpha = 1.400000, \beta = 0.300000$ ***Figure 7***
Map = 1, P = 1, N = 200000, I = 100
$(x,y) \in [-2.000000,2.000000] \times [-2.000000,2.000000]$

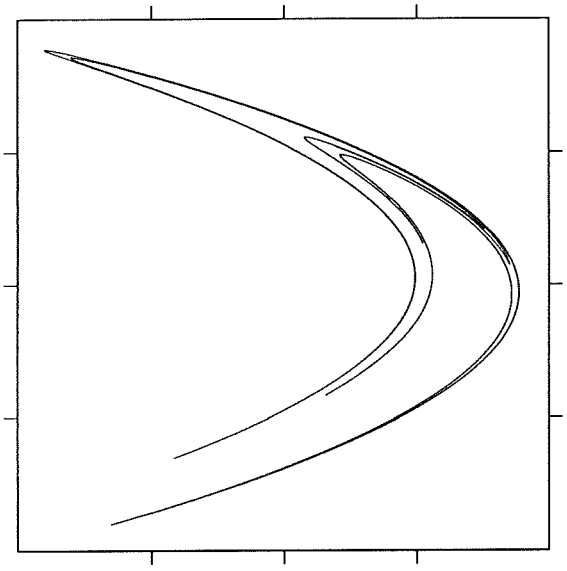

$\alpha = 1.560000, \beta = 0.400000$ ***Figure 8***
Map = 2, P = 1, N = 200000, I = 100
$(x,y) \in [-2.500000,2.500000] \times [-2.500000,2.500000]$

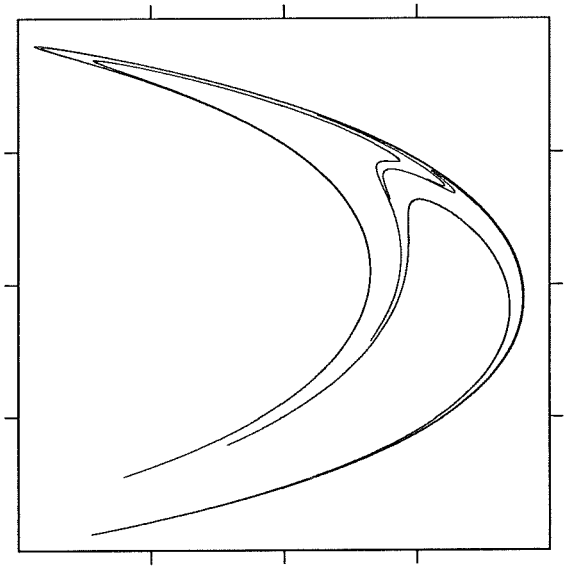

$\alpha = 10.400000, \beta = 0.300000$ ***Figure 9***
Map = 3, P = 1, N = 200000, I = 100
$(x,y) \in [-14.000000,14.000000] \times [-14.000000,14.000000]$

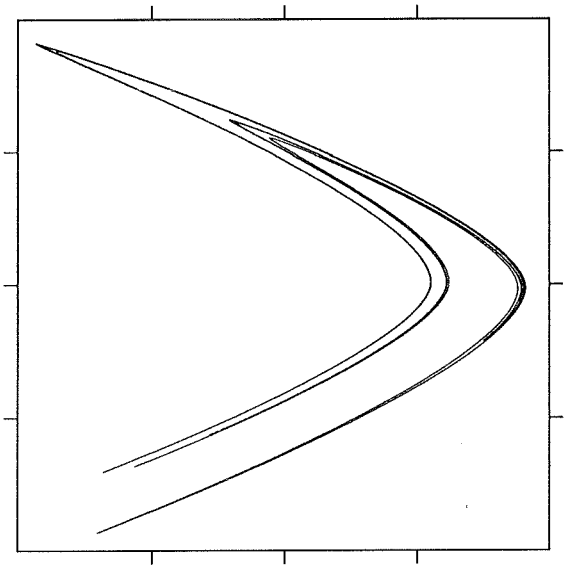

$\alpha = 1.410000, \beta = 0.300000$ ***Figure 10***
Map = 4, P = 1, N = 200000, I = 100
$(x,y) \in [-2.000000,2.000000] \times [-2.000000,2.000000]$

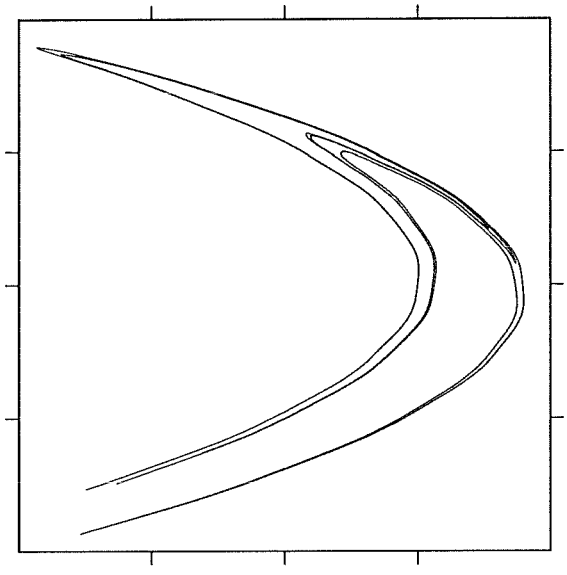

$\alpha = 2.100000, \beta = 0.400000$ ***Figure 11***
Map = 5, P = 1, N = 200000, I = 100
$(x,y) \in [-3.250000,3.250000] \times [-3.250000,3.250000]$

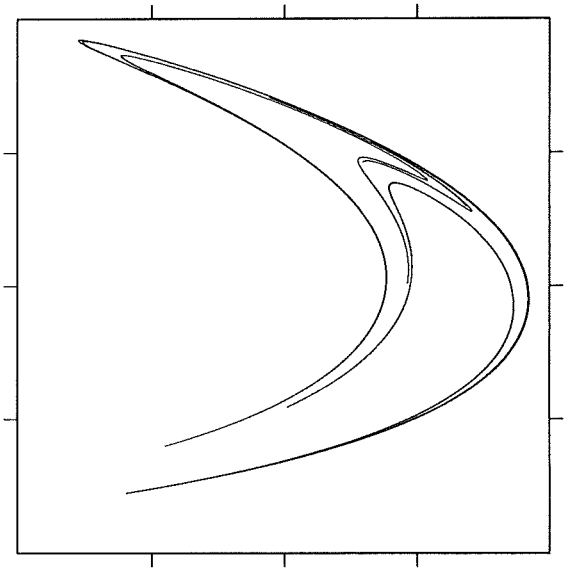

$\alpha = 1.550000, \beta = 0.300000$ ***Figure 12***
Map = 6, P = 1, N = 200000, I = 100
$(x,y) \in [-2.000000,2.000000] \times [-2.000000,2.000000]$

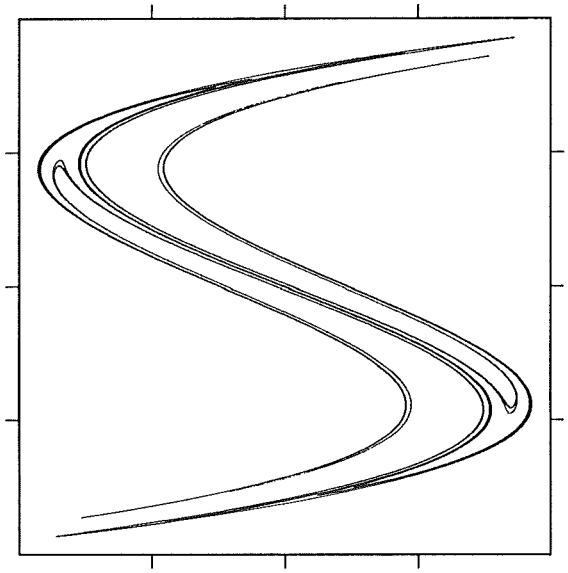

$\alpha = 1.400000$, $\beta = 0.300000$ ***Figure 13***
Map = 1, P = 500, N = 2000, I = 100
$(x,y) \in [0.850000,0.900000] \times [0.850000,0.900000]$

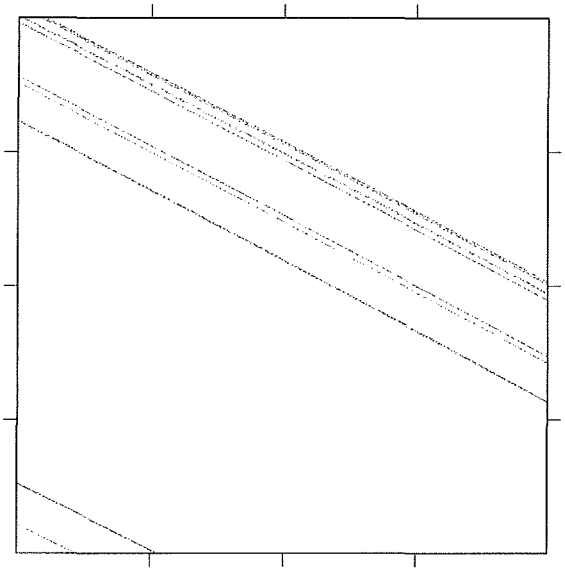

$\alpha = 1.400000$, $\beta = 0.300000$ ***Figure 14***
Map = 1, P = 1000, N = 4000, I = 100
$(x,y) \in [0.875000,0.885000] \times [0.875000,0.885000]$

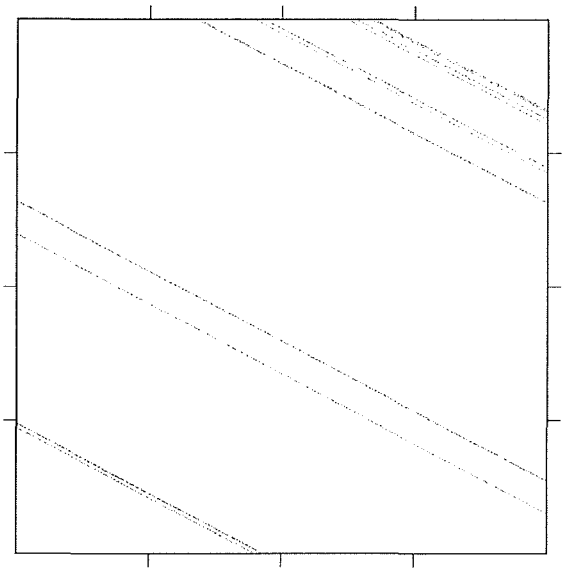

$\alpha = 1.560000$, $\beta = 0.400000$ ***Figure 15***
Map = 2, P = 500, N = 2000, I = 100
$(x,y) \in [1.100000,1.300000] \times [1.100000,1.300000]$

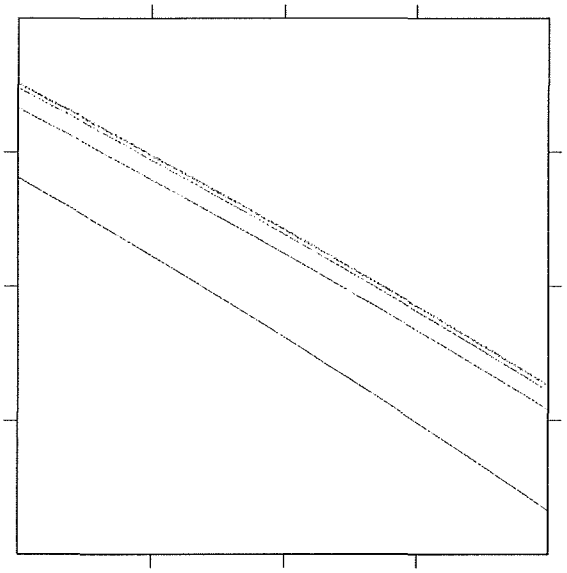

$\alpha = 1.560000$, $\beta = 0.400000$ ***Figure 16***
Map = 2, P = 1000, N = 4000, I = 100
$(x,y) \in [1.200000,1.220000] \times [1.200000,1.220000]$

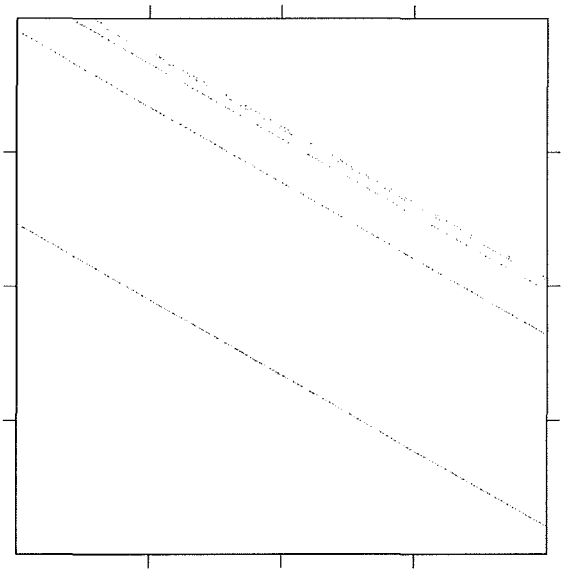

$\alpha = 10.400000$, $\beta = 0.300000$ ***Figure 17***
Map = 3, P = 500, N = 2000, I = 100
$(x,y) \in [5.200000,5.600000] \times [5.200000,5.600000]$

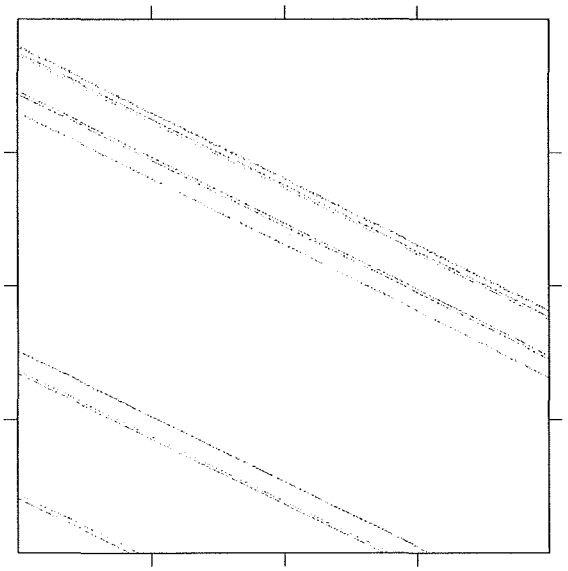

$\alpha = 10.400000$, $\beta = 0.300000$ ***Figure 18***
Map = 3, P = 1000, N = 4000, I = 100
$(x,y) \in [5.400000,5.500000] \times [5.400000,5.500000]$

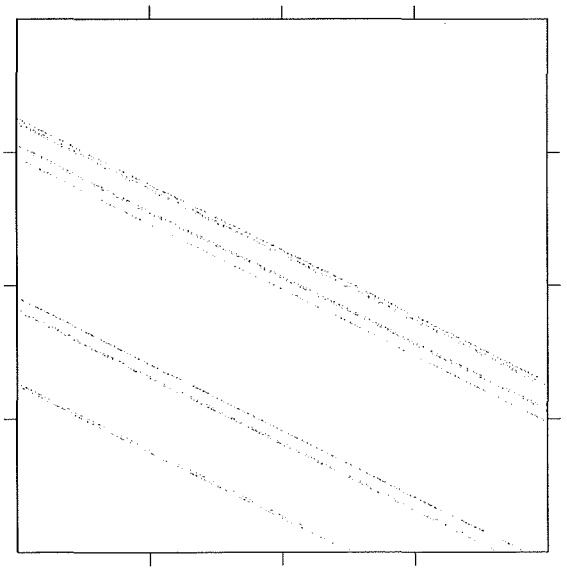

$\alpha = 1.410000$, $\beta = 0.300000$ ***Figure 19***
Map = 4, P = 500, N = 2000, I = 100
$(x,y) \in [0.800000,0.950000] \times [0.800000,0.950000]$

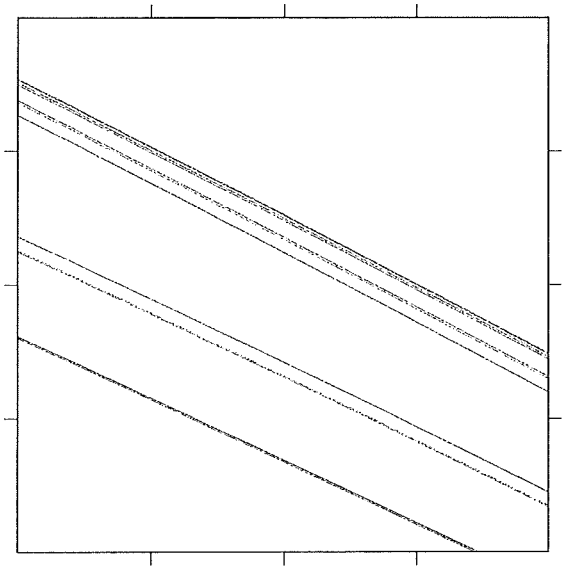

$\alpha = 1.410000$, $\beta = 0.300000$ ***Figure 20***
Map = 4, P = 1000, N = 4000, I = 100
$(x,y) \in [0.860000,0.900000] \times [0.860000,0.900000]$

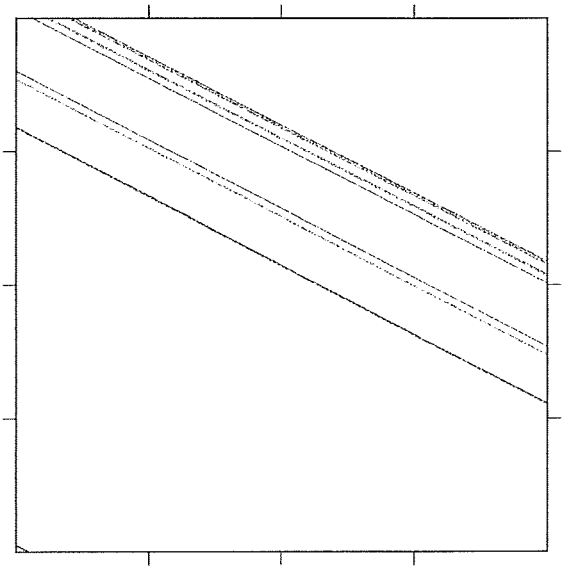

$\alpha = 2.100000$, $\beta = 0.400000$ ***Figure 21***
Map = 5, P = 500, N = 2000, I = 100
$(x,y) \in [1.400000,1.600000] \times [1.400000,1.600000]$

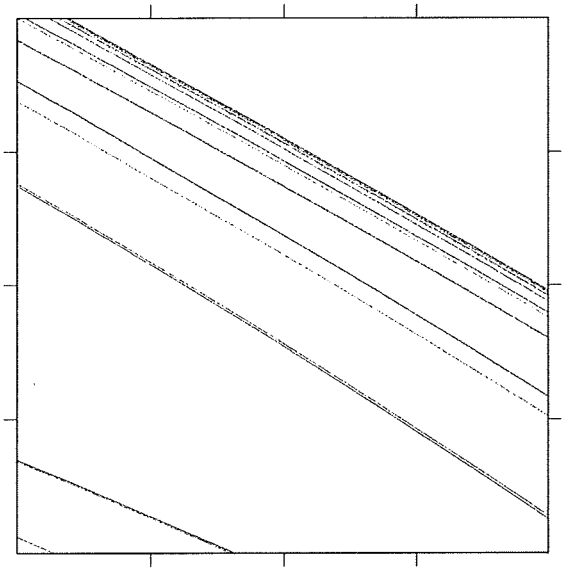

$\alpha = 2.100000$, $\beta = 0.400000$ ***Figure 22***
Map = 5, P = 1000, N = 4000, I = 100
$(x,y) \in [1.500000,1.550000] \times [1.500000,1.550000]$

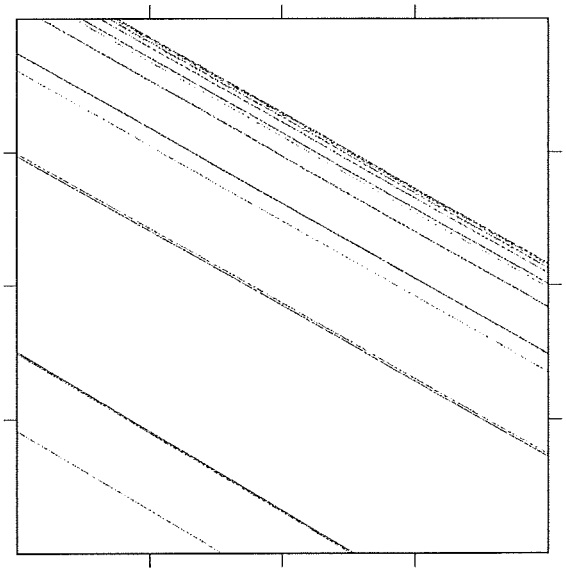

$\alpha = 1.550000$, $\beta = 0.300000$ ***Figure 23***
Map = 6, P = 500, N = 2000, I = 100
$(x,y) \in [1.600000,1.900000] \times [1.600000,1.900000]$

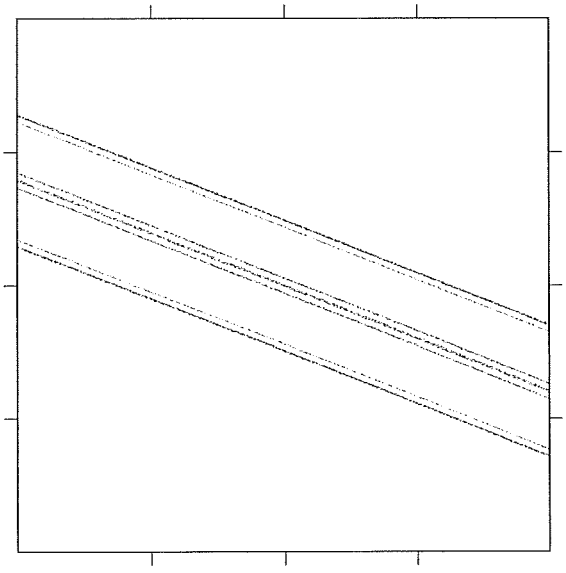

$\alpha = 1.550000$, $\beta = 0.300000$ ***Figure 24***
Map = 6, P = 1000, N = 4000, I = 100
$(x,y) \in [1.700000,1.800000] \times [1.700000,1.800000]$

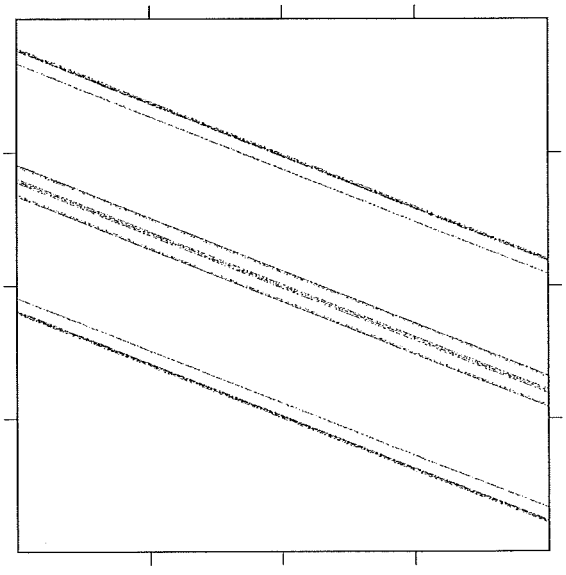

$\alpha = 1.400000$, $\beta = 0.300000$ ***Figure 25***
Map = 1, P = 30, N = 200, I = 100
$(x,y) \in [-5.000000,5.000000] \times [-5.000000,5.000000]$

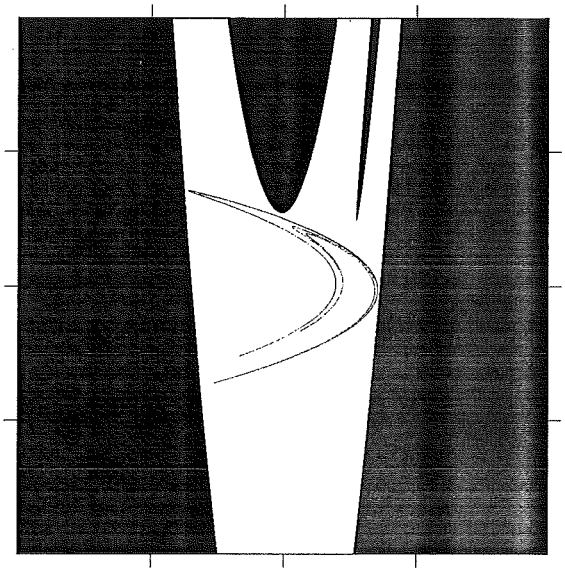

$\alpha = 1.560000$, $\beta = 0.400000$ ***Figure 26***
Map = 2, P = 30, N = 200, I = 100
$(x,y) \in [-5.000000,5.000000] \times [-5.000000,5.000000]$

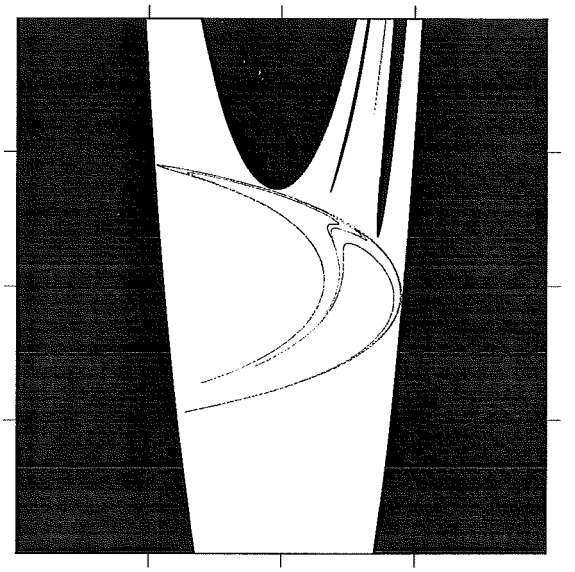

$\alpha = 10.400000$, $\beta = 0.300000$ ***Figure 27***
Map = 3, P = 30, N = 200, I = 100
$(x,y) \in [-16.000000,16.000000] \times [-16.000000,16.000000]$

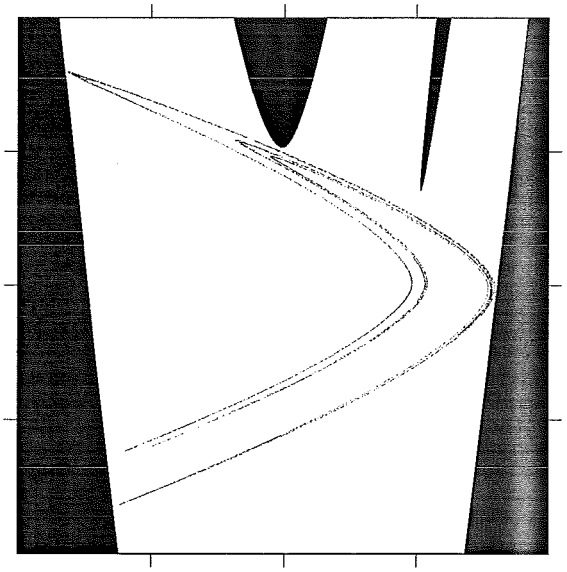

$\alpha = 1.410000$, $\beta = 0.300000$ ***Figwre 28***
Map = 4, P = 30, N = 200, I = 100
$(x,y) \in [-5.000000,5.000000] \times [-5.000000,5.000000]$

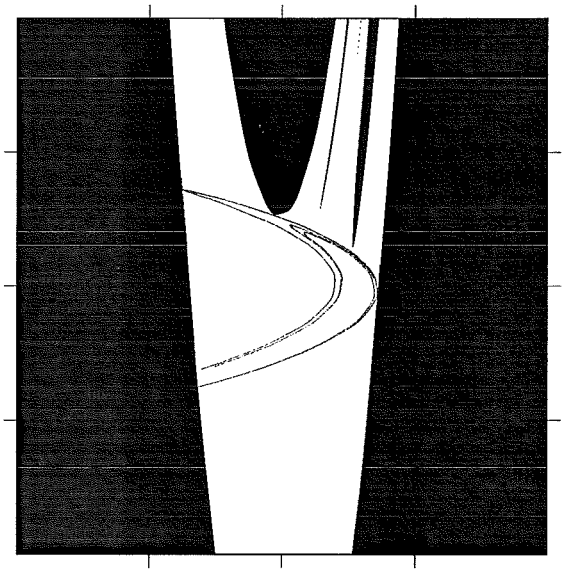

$\alpha = 2.100000$, $\beta = 0.400000$ ***Figure 29***
Map = 5, P = 30, N = 200, I = 100
$(x,y) \in [-6.000000,6.000000] \times [-6.000000,6.000000]$

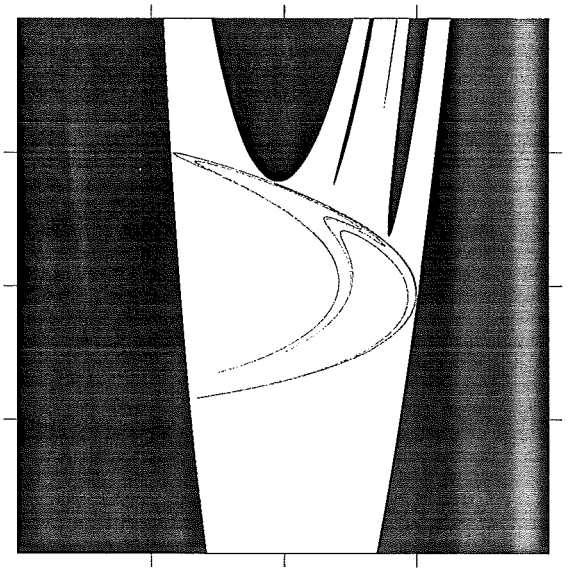

$\alpha = 1.550000$, $\beta = 0.300000$ ***Figure 30***
Map = 6, P = 30, N = 200, I = 100
$(x,y) \in [-6.000000,6.000000] \times [-6.000000,6.000000]$

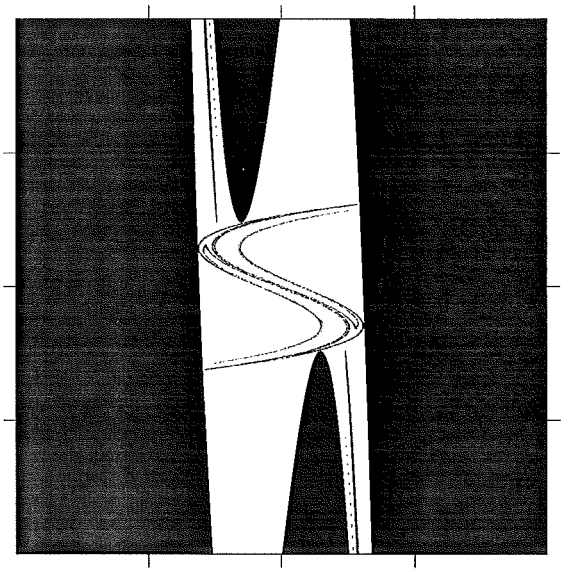

(x,y) = (0.100000,0.050000) ***Figure 31***
β = 0.300000 Map = 1, I = 400, P = 1000
(α,L)∈ [1.390000,1.410000]×[0.000000,1.000000]

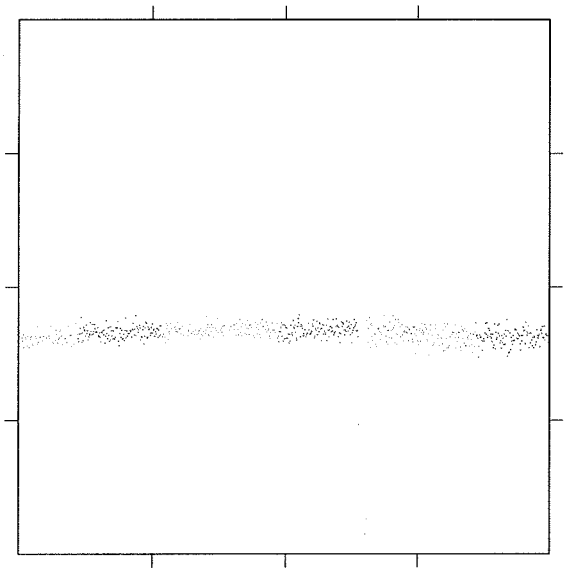

(x,y) = (0.100000,0.050000) ***Figure 32***
β = 0.400000 Map = 2, I = 400, P = 1000
(α,L)∈ [1.550000,1.570000]×[0.000000,1.000000]

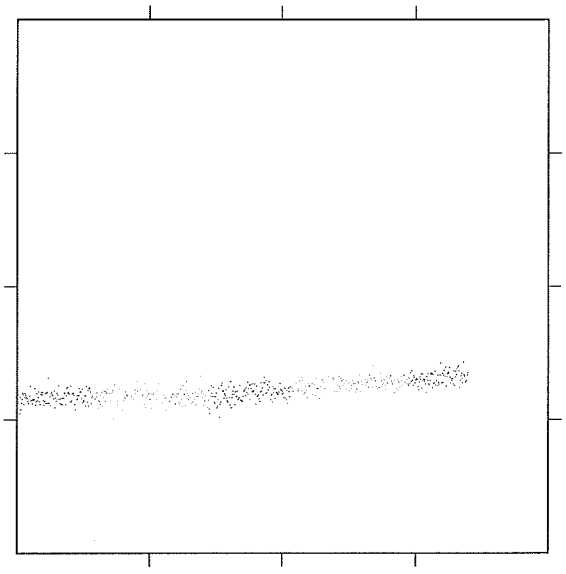

(x,y) = (0.100000,0.050000) ***Figure 33***
β = 0.300000 Map = 3, I = 400, P = 1000
(α,L)∈ [10.300000,10.500000]×[0.000000,1.000000]

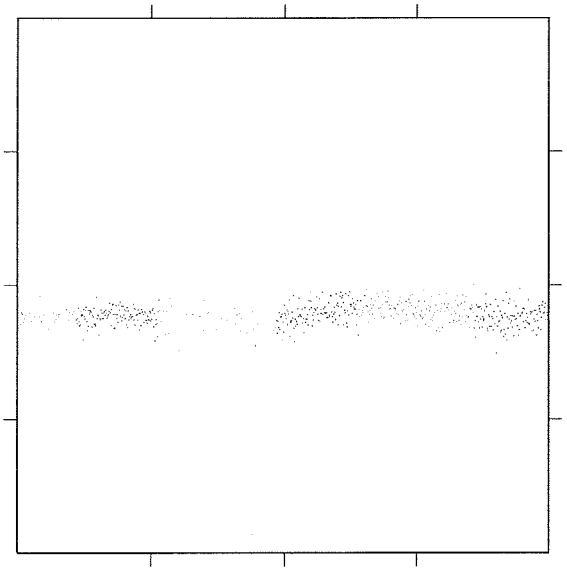

(x,y) = (0.100000,0.050000) ***Figure 34***
β = 0.300000 Map = 4, I = 400, P = 1000
(α,L)∈ [1.400000,1.420000]×[0.000000,1.000000]

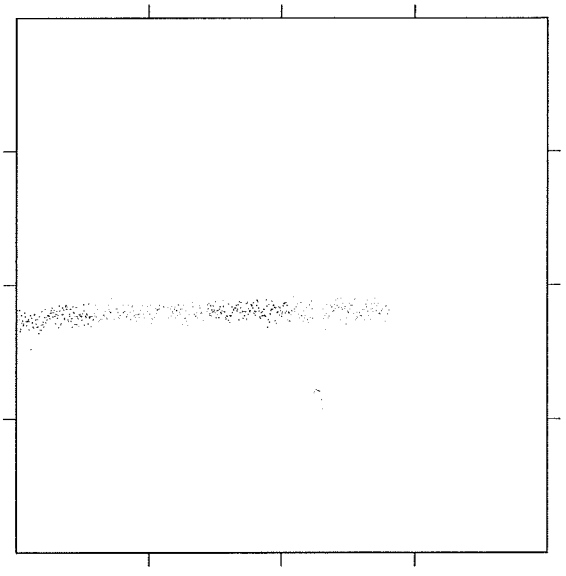

(x,y) = (0.100000,0.050000) ***Figure 35***
β = 0.400000 Map = 5, I = 400, P = 1000
(α,L)∈ [2.090000,2.110000]×[0.000000,1.000000]

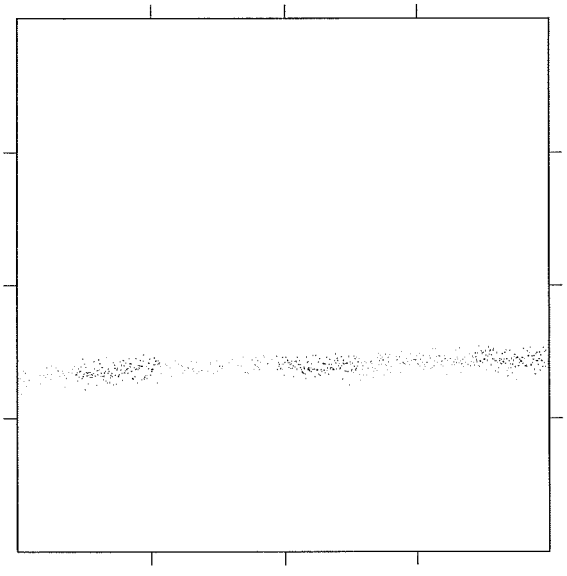

(x,y) = (0.100000,0.050000) ***Figure 36***
β = 0.300000 Map = 6, I = 400, P = 1000
(α,L)∈ [1.540000,1.560000]×[0.000000,1.000000]

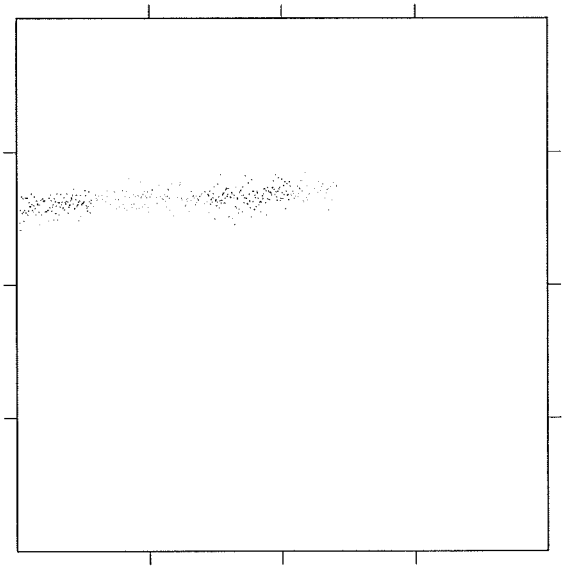

(x,y) = (0.100000,0.200000) ***Figure 37***
α = 1.400000 Map = 1, I = 400, P = 1000
(β,L)∈ [0.299000,0.301000]×[0.000000,1.000000]

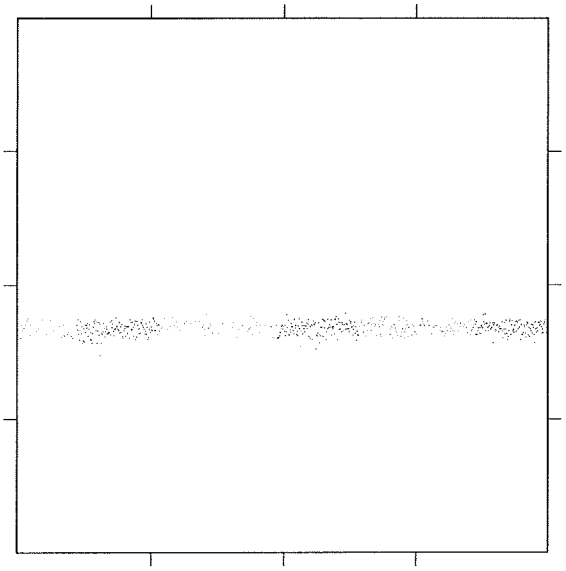

(x,y) = (0.100000,0.200000) ***Figure 38***
α = 1.560000 Map = 2, I = 400, P = 1000
(β,L)∈ [0.399000,0.401000]×[0.000000,1.000000]

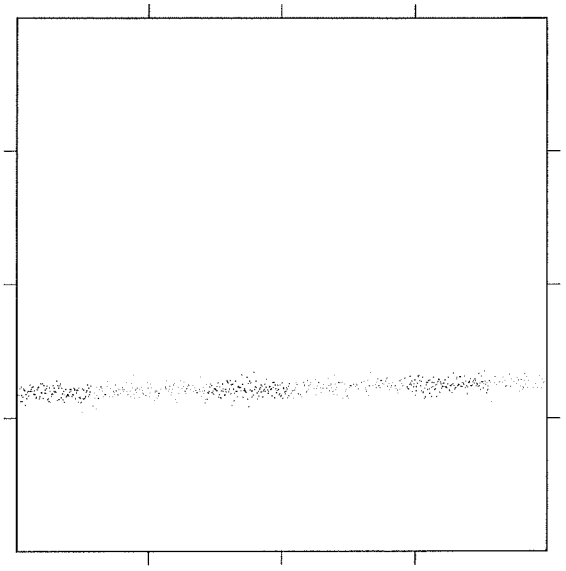

(x,y) = (0.100000,0.200000) ***Figure 39***
α = 10.400000 Map = 3, I = 400, P = 1000
(β,L)∈ [0.295000,0.305000]×[0.000000,1.000000]

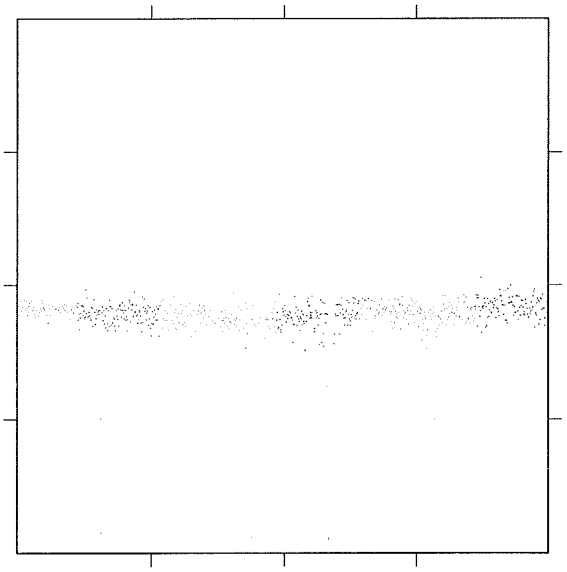

(x,y) = (0.100000,0.200000) ***Figure 40***
α = 1.410000 Map = 4, I = 400, P = 1000
(β,L)∈ [0.299000,0.301000]×[0.000000,1.000000]

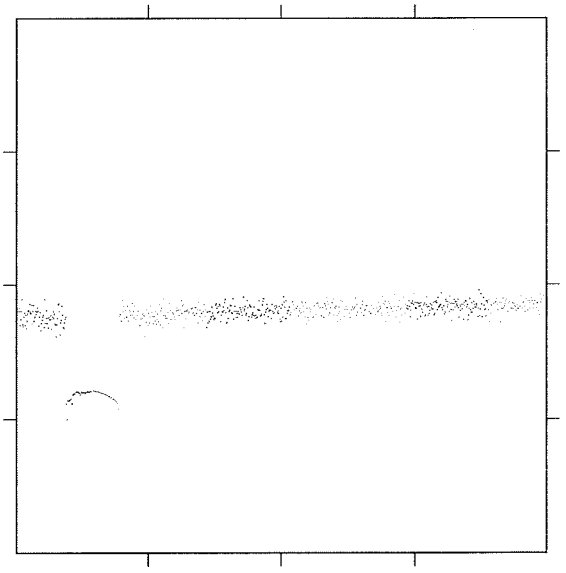

(x,y) = (0.100000,0.200000) ***Figure 41***
α = 2.100000 Map = 5, I = 400, P = 1000
(β,L)∈ [0.399000,0.401000]×[0.000000,1.000000]

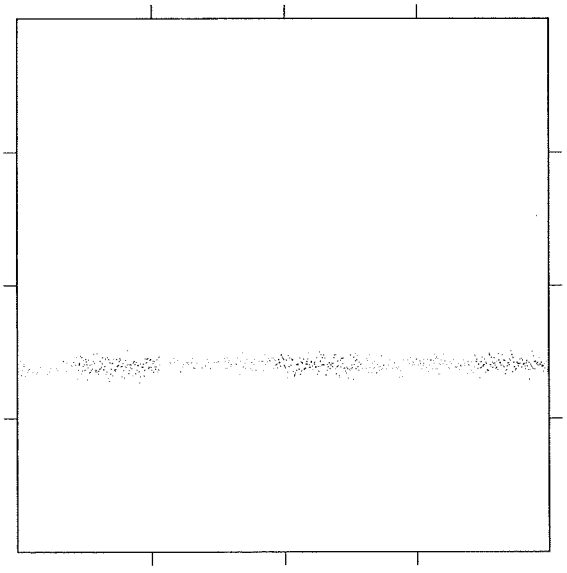

(x,y) = (0.100000,0.200000) ***Figure 42***
α = 1.550000 Map = 6, I = 400, P = 1000
(β,L)∈ [0.299000,0.301000]×[0.000000,1.000000]

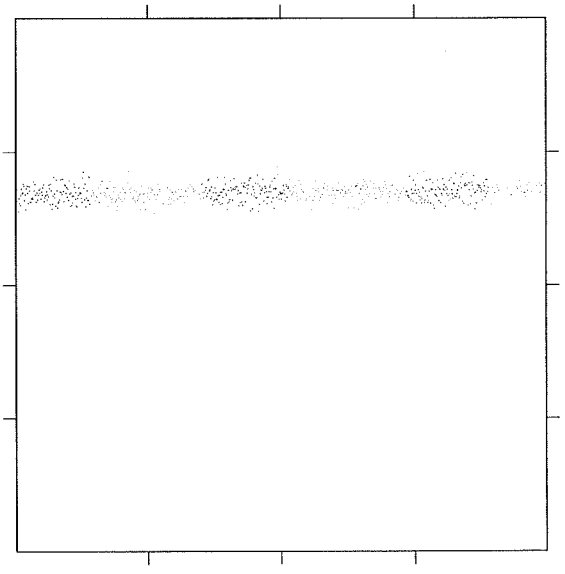

(x,y) = (0.200000,0.200000) ***Figure 43***
β = 0.217000 Map = 1, I = 400, P = 1500
(α,x)∈ [1.520000,1.550000]×[−1.153800,−0.908000]

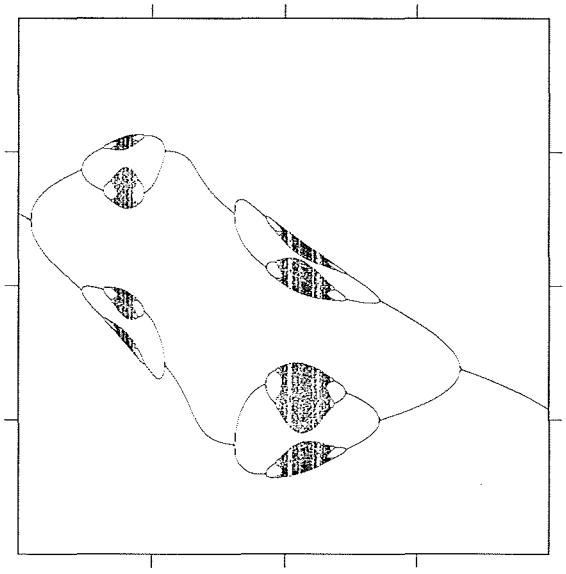

(x,y) = (0.200000,0.200000) ***Figure 44***
β = 0.150000 Map = 2, I = 400, P = 1500
(α,x)∈ [2.095400,2.108130]×[1.811210,1.861590]

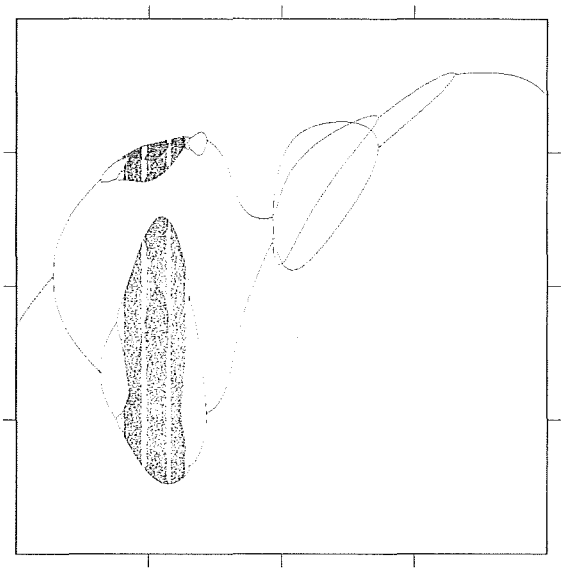

(x,y) = (0.200000,0.200000) ***Figure 45***
β = 0.201000 Map = 3, I = 400, P = 1500
(α,x)∈ [8.211250,8.573100]×[−1.228000,−0.775000]

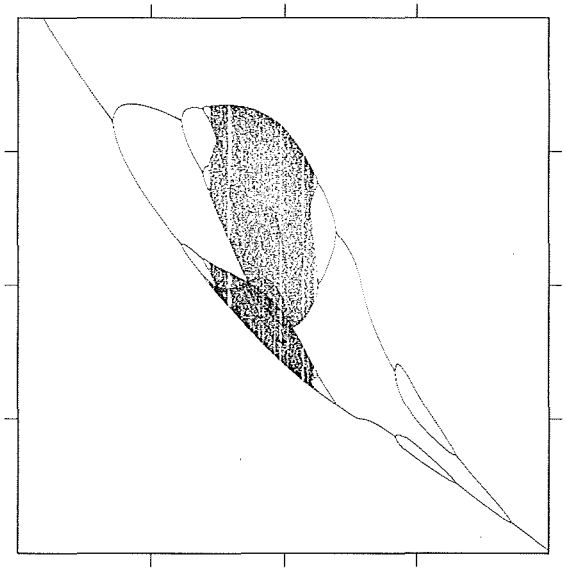

(x,y) = (0.200000,0.200000) ***Figure 46***
β = 0.170110 Map = 4, I = 400, P = 1500
(α,x)∈ [1.599000,1.603000]×[−1.394000,−1.354800]

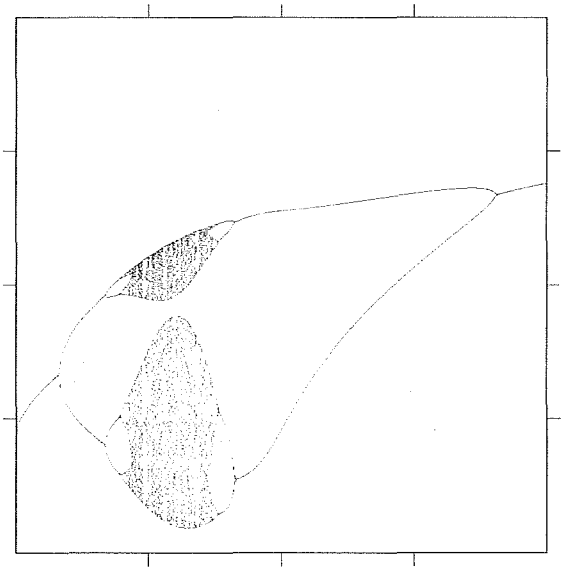

(x,y) = (0.200000,0.200000) ***Figure 47***
β = 0.349900 Map = 5, I = 400, P = 1500
(α,x)∈ [2.055800,2.056300]×[1.123000,1.130000]

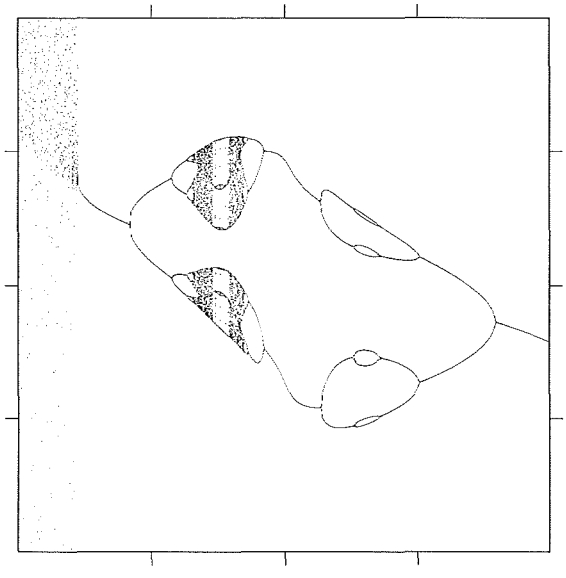

(x,y) = (0.200000,0.200000) ***Figure 48***
β = 0.129800 Map = 6, I = 400, P = 1500
(α,x)∈ [1.485280,1.493630]×[−1.180000,−0.618000]

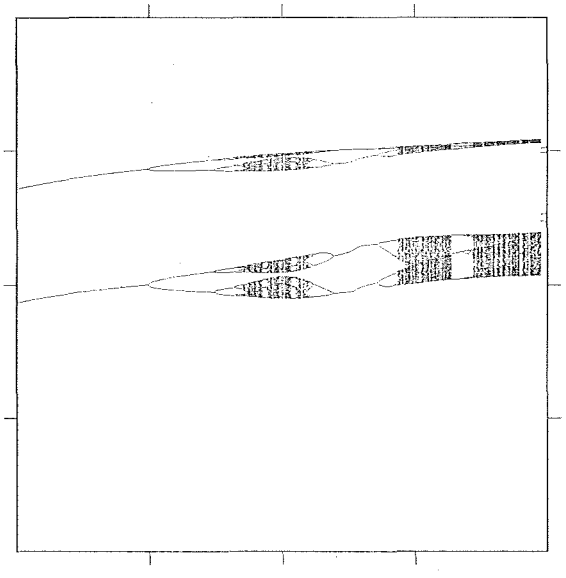

9. An example of a map with a hyperbolic horseshoe with three symbols

Let $g : \mathbb{R} \longrightarrow \mathbb{R}$ be any differentiable map. The formula

$$F(x,y) = (f(x) + \beta y, x)$$

"lifts" the map to a diffeomorphism of $\mathbb{R}^2$, with inverse

$$F^{-1}(x,y) = \big(y, \beta^{-1}(x - f(y))\big)$$

if $\beta \neq 0$. For small epsilon we might hope that some of the properties of the one-dimensional map carry over to the diffeomorphism. This is in fact the case and will be proven elsewhere. We will here however consider a particular example.

Consider the one-dimensional system $x \mapsto f_\alpha(x)$ where $f_\alpha(x) = x^3 - \alpha^2 x$ and $\alpha \geq 0$. It is easily seen that the following is true for this family:

Simple properties of a qubic family. *Let $f_\alpha(x) = x^3 - \alpha^2 x$ and $\alpha \geq 0$. Then the following holds for the corresponding one-dimensional dynamical system:*

1. *f_α has three fixed-points given by $x_1 = -\sqrt{\alpha^2+1}$, $x_2 = 0$ and $x_3 = \sqrt{\alpha^2+1}$. x_1 and x_3 are always unstable. x_2 is stable for $\alpha < 1$ and unstable for $\alpha > 1$.*
2. *$\Omega(f_\alpha) \subset I_\Omega(\alpha) = [-\sqrt{\alpha^2+1}, \sqrt{\alpha^2+1}]$. $I_\Omega(\alpha)$ is the smallest closed interval containing $\Omega(f_\alpha)$. If $\alpha \leq \sqrt{3}$ $I_\Omega(\alpha)$ is invariant in the sense that $f(I_\Omega(\alpha)) \subset I_\Omega(\alpha)$.*
3. *For $0 \leq \alpha \leq 1$ $\Omega(f_\alpha) = \{x_1, x_2, x_3\}$.*
4. *At $\alpha = \sqrt{3}$ the fixed points x_1 and x_2 becomes snap-back repellors (f_α has a homoclinic bifurcation at $\alpha = \sqrt{3}$), and hetroclinic orbits connecting x_1 and x_3 are born at this parameter-value.*
5. *f_α restricted to $\Omega(f_\alpha)$ is topologically equivalent to $\sigma : \Sigma_3^+ \longrightarrow \Sigma_3^+$ for $\alpha > \sqrt{3}$.*
6. *$\Omega(f_\alpha)$ is hyperbolic if $\alpha > \sqrt{\dfrac{1+3\sqrt{3}}{2}}$.*

Proof. The assumption $\alpha \geq 0$ is motivated from the fact that $f(x,\alpha)$ is even in α, $f(x,\alpha) = f(x,-\alpha)$. $f(x,\alpha)$ is an odd function in x, $f(-x,\alpha) = -f(x,\alpha)$, and this symmetry will be used in the following without explicit reference to this property.

(1) The fixed-points are found by solving $f_\alpha(x) = x$. The equation $x^2 - \alpha^2 = x$ has three solutions, $x_1 = -\sqrt{\alpha^2+1}$, $x_2 = 0$ and $x_3 = \sqrt{\alpha^2+1}$. The derivative of f_α is $f'_\alpha(x) = 3x^2 - \alpha^2$. We find that $f'_\alpha(x_1) = f'_\alpha(x_3) = 2\alpha^2 + 3 \geq 3 > 1$ for all α so x_1 and x_3 is unstable. $f'_\alpha(x_2) = -\alpha^2$ so $|f'_\alpha(x_2)| < 1$ if $|\alpha| < 1$ and $|f'_\alpha(x_2)| > 1$ if $|\alpha| > 1$, so x_1 is stable for $|\alpha| < 1$ and unstable for $|\alpha| > 1$.

(2) $f_\alpha(x) > x$ for $x > \sqrt{\alpha^2+1}$ and $f_\alpha(x) < x$ for $x < -\sqrt{\alpha^2+1}$. By lemma 5

$$\Omega(f_\alpha) \cap \Big(\mathbb{R} \setminus (-\sqrt{\alpha^2+1}, \sqrt{\alpha^2+1})\Big) = \varnothing$$

so $\Omega(f_\alpha) \subset I_\Omega(\alpha) = [-\sqrt{\alpha^2+1}, \sqrt{\alpha^2+1}]$. The endpoints of this interval are fixed-points and therefore in $\Omega(f_\alpha)$. Hence $I_\Omega(\alpha)$ is the smallest closed interval containing $\Omega(f_\alpha)$. The zeroes of $f'_\alpha(x) = 0$ are given by $x_{c_1} = -\alpha/\sqrt{3}$ and $x_{c_2} = \alpha/\sqrt{3}$. The image of x_{c_1} is $f_\alpha(x_{c_1}) = -f_\alpha(x_{c_2}) = 2\alpha^3/\sqrt{3}$. Clearly $2\alpha^3/\sqrt{3} < \sqrt{\alpha^2+1}$ if $|\alpha| < \sqrt{3}$, $2\alpha^3/\sqrt{3} = \sqrt{\alpha^2+1}$ if $|\alpha| = \sqrt{3}$ and $2\alpha^3/\sqrt{3} > \sqrt{\alpha^2+1}$ if $|\alpha| > \sqrt{3}$, so $f_\alpha(I_\Omega(\alpha)) \subset I_\Omega(\alpha)$ if $|\alpha| \leq \sqrt{3}$.

(3) If $0 \leq \alpha \leq 1$, $x \in (-\sqrt{\alpha^2+1}, \sqrt{\alpha^2+1})$ and $x \neq 0$ we see that $-|x| < f_\alpha(x) < |x|$ so for any $x \in (-\sqrt{\alpha^2+1}, \sqrt{\alpha^2+1})$ we have $\omega(x, f_\alpha) = x_2 = 0$. Then, by (2), $\Omega(f_\alpha) = \{x_1, x_2, x_3\}$.

(4) At $\alpha = \sqrt{3}$ we see that $f_{\sqrt{3}}(x_{c_1}) = x_3$ and $f_{\sqrt{3}}(x_{c_2}) = x_1$. Consider the preimages of x_{c_1} and x_{c_2}, that is, the solutions of $f_{\sqrt{3}}(x) = x_{c_1}$ and $f_{\sqrt{3}}(x) = x_{c_1}$. It is easily seen that $f^{-1}_{\sqrt{3}}(\{x_{c_1}\}) = \{-2\cos\frac{\pi}{9}, \cos\frac{\pi}{9} + \sqrt{3}\sin\frac{\pi}{9}, \cos\frac{\pi}{9} - \sqrt{3}\sin\frac{\pi}{9}\}$ and $f^{-1}_{\sqrt{3}}(\{x_{c_2}\}) = \{2\cos\frac{\pi}{9}, -\cos\frac{\pi}{9} - \sqrt{3}\sin\frac{\pi}{9}, -\cos\frac{\pi}{9} +$

$\sqrt{3}\sin\frac{\pi}{9}\}$. We see that $\cos\frac{\pi}{9}+\sqrt{3}\sin\frac{\pi}{9} > x_{c_2} = 1$. f restricted to the interval $[\cos\frac{\pi}{9}+\sqrt{3}\sin\frac{\pi}{9}, 2]$ is invertible. Let g denote the inverse map on this interval. It is easily seen that $x_3 = 2$ is an attractive fixed point for g. This proves the existence of a homoclinic orbit for x_3. The other statements in (4) are proved in a similar manner. To see that $\alpha = \sqrt{3}$ is a bifurcation value we note that $f_\alpha^{-1}(\{x_1\})$ and $f_\alpha^{-1}(\{x_3\})$ are single points for $\alpha < \sqrt{3}$.

(5) If $\alpha > \sqrt{3}$ we observe that there exist three disjoint closed intervals I_1, I_2 and I_3 in $[x_1, x_3]$ such that $f_\alpha(I_i) = [x_1, x_3]$, $i = 1, 2, 3$. We then construct a Cantor set in the usual manner by removing two open intervals on each sublevel of the construction. Each point in this Cantor set may be described by a infinite sequence of three symbols, and we establish a homeomorphism from the non-wandering set to the symbol space as for the logistic family.

(6) To find the parameter value where the Cantor set from (5) become a hyperbolic set we first find the three intervals I_1, I_2 and I_3 in $[x_1, x_3]$ from (5). The endpoints of these intervals are the preimages of x_1 and x_3. Then we find the parametervalue such that $|f'_\alpha(x)| > 1$ for $x \in I_1 \cup I_2 \cup I_3$. Note that $x^3-\alpha^2x-\sqrt{\alpha^2+1} = (x-\sqrt{\alpha^2+1})(x-\frac{1}{2}(\sqrt{\alpha^2-3}-\sqrt{\alpha^2+1}))(x-\frac{1}{2}(\sqrt{\alpha^2-3}+\sqrt{\alpha^2+1}))$. By symmetry the intervals are given by

$$I_1 = [-\sqrt{\alpha^2+1}, -\frac{1}{2}(\sqrt{\alpha^2-3}+\sqrt{\alpha^2+1})] = [x_1, x_{h_1}]$$
$$I_2 = [-\frac{1}{2}(\sqrt{\alpha^2-3}-\sqrt{\alpha^2+1}), \frac{1}{2}(\sqrt{\alpha^2-3}-\sqrt{\alpha^2+1})] = [x_{h_2}, x_{h_3}]$$
$$I_3 = [\frac{1}{2}(\sqrt{\alpha^2-3}+\sqrt{\alpha^2+1}), \sqrt{\alpha^2+1}] = [x_{h_4}, x_3].$$

We will now find an α_h such that $|f'_\alpha(x)| > 1$ for $x \in I_1 \cup I_2 \cup I_3$. By the properties of f_α it is sufficient to find an α_h such that $f'_\alpha(x_{h_1}) > 1$ and $f'_\alpha(x_{h_2}) < -1$ if $\alpha > \alpha_h$. By solving the equation $f'_\alpha(x_{h_1}) = 1$ we obtain the equation $2\alpha^4-2\alpha^2-13 = 0$, and hence $\alpha_{h_1} = \sqrt{\frac{1+3\sqrt{3}}{2}}$. By solving the equation $f'_\alpha(x_{h_2}) = -1$ we obtain the equation $2\alpha^4-4\alpha^2-7 = 0$, and hence $\alpha_{h_2} = \sqrt{\frac{2+3\sqrt{2}}{2}}$. Let $\alpha_h = \max\{\alpha_{h_1}, \alpha_{h_2}\} = \sqrt{\frac{1+3\sqrt{3}}{2}}$, and it follows that $\Omega(f_\alpha)$ is hyperbolic if $\alpha > \sqrt{\frac{1+3\sqrt{3}}{2}}$.

We will now look at some simple properties of the lifted system. In the following we assume $\alpha \geq 0$ and $|\beta| < 1$.

FIXED POINT IN THE LIFTED SYSTEM. The fixed point in $(x, y) \mapsto (x^3 - \alpha^2 x + \beta x, x)$ is found by solving the equation $(x^3-\alpha^2x+\beta x, x) = (x, y)$. The solutions are given by $p_1 = (-\sqrt{\alpha^2+1-\beta}, -\sqrt{\alpha^2+1-\beta})$, $p_2 = (0, 0)$ and $p_3 = (\sqrt{\alpha^2+1-\beta}, \sqrt{\alpha^2+1-\beta})$. The eigenvalues of the Jacobi matrix at p_1 and p_3 is given by

$$\lambda_1 = \frac{3+2\alpha^2-3\beta+\sqrt{9+12\alpha^2+4\alpha^4-14\beta-12\alpha^2\beta+9\beta^2}}{2}$$
$$\lambda_2 = \frac{3+2\alpha^2-3\beta-\sqrt{9+12\alpha^2+4\alpha^4-14\beta-12\alpha^2\beta+9\beta^2}}{2}.$$

The eigenvalues of the Jacobi matrix at p_2 is given by

$$\lambda_1 = \frac{-\alpha^2+\sqrt{\alpha^4+4\beta}}{2}$$
$$\lambda_2 = \frac{-\left(\alpha^2+\sqrt{\alpha^4+4\beta}\right)}{2}$$

It is easily seen that p_1 and p_3 has an eigenvalue 1 on the parabola $\beta = 1+\alpha^2$ and an eigenvalue -1 on the parabola $\beta = 1+\alpha^2/2$. Hence p_1 and p_3 are hyperbolic saddles for $|\beta| < 1$. p_2 has an eigenvalue 1 on the parabola $\beta = 1+\alpha^2$ and an eigenvalue -1 on the parabola $\beta = 1-\alpha^2$. Hence p_2 is an attracting fixed point if $0 \leq \alpha(\beta) < \sqrt{1-\beta}$, and a hyperbolic saddle if $\alpha(\beta) > \sqrt{1-\beta}$. We remark that at $\alpha(\beta) = \sqrt{1-\beta}$ there is a period doubling bifurcation at p_2 where a period-2 orbit is born.

APPROXIMATION OF THE NON-WANDERING SET OF THE LIFTED SYSTEM. We will show that $\mathbf{\Omega}(F_{\alpha,\beta})$ is contained in a square $[-R,R]^2$ by a similar method to what we used in section 5. Let $R>0$ and let $\mathcal{S}(R)$ be the square with vertices $A=(-R,-R)$, $B=(R,-R)$, $C=(R,R)$ and $D=(-R,R)$. We define

$$\begin{aligned}
M_1(R) &= \{(x,y)\in\mathbb{R}^2 : x\geq R, |y|\leq x\}\\
M_2(R) &= \{(x,y)\in\mathbb{R}^2 : y\geq R, |x|\leq y\}\\
M_3(R) &= \{(x,y)\in\mathbb{R}^2 : x\leq -R, |y|\leq -x\}\\
M_4(R) &= \{(x,y)\in\mathbb{R}^2 : y\leq -R, |x|\leq -y\}.
\end{aligned}$$

Clearly $M_1\cup M_2\cup M_3\cup M_4=\mathbb{R}^2\setminus(\text{int }(\mathcal{S}(R)))$. Let Δ^+ and Δ^- be the diagonal and the antidiagonal in $\mathbb{R}^2$, and let Δ_R^+ denote the two halflines with $|x|\geq R$ in Δ^+. Δ_R^- is defined similarly. The sets $F_{\alpha,\beta}(\Delta^+)$, $F_{\alpha,\beta}(\Delta^-)$, $F_{\alpha,\beta}^{-1}(\Delta^+)$ and $F_{\alpha,\beta}^{-1}(\Delta^-)$ are all qubic curves, and it is easily seen that $F_{\alpha,\beta}(\Delta_R^+)\cup F_{\alpha,\beta}(\Delta_R^-)\subset M_1(R)\cup M_3(R)$, and $F_{\alpha,\beta}^{-1}(\Delta_R^+)\cup F_{\alpha,\beta}^{-1}(\Delta_R^-)\subset M_2(R)\cup M_4(R)$ for R large enough. Since vertical line segments are mapped to horizontal line segments by $F_{\alpha,\beta}$ and horizontal line segments are mapped to vertical line segments by $F_{\alpha,\beta}^{-1}$, we see that if $\beta>0$ then $F_{\alpha,\beta}(M_1(R))\subset$ int $(M_1(R)$ if $\pi_1(F_{\alpha,\beta}(B))>R$, $F_{\alpha,\beta}(M_3(R))\subset$ int $(M_3(R)$ if $\pi_1(F_{\alpha,\beta}(D))<-R$, $F_{\alpha,\beta}^{-1}(M_2(R))\subset$ int $(M_4(R)$ if $\pi_2(F_{\alpha,\beta}^{-1}(C))<-R$ and $F_{\alpha,\beta}^{-1}(M_4(R))\subset$ int $(M_2(R)$ if $\pi_2(F_{\alpha,\beta}^{-1}(A))>R$. In all four cases we get the inequality

$$R^3-\alpha^2R-(\beta+1)R>0.$$

Clearly this inequality holds for all $R>\sqrt{\alpha^2+\beta+1}$. For $\beta<0$ we see that $F_{\alpha,\beta}(M_1(R))\subset$ int $(M_1(R)$ if $\pi_1(F_{\alpha,\beta}(C))>R$, $F_{\alpha,\beta}(M_3(R))\subset$ int $(M_3(R)$ if $\pi_1(F_{\alpha,\beta}(A))<-R$, $F_{\alpha,\beta}^{-1}(M_2(R))\subset$ int $(M_2(R)$ if $\pi_2(F_{\alpha,\beta}^{-1}(C))>R$ and $F_{\alpha,\beta}^{-1}(M_4(R))\subset$ int $(M_4(R)$ if $\pi_2(F_{\alpha,\beta}^{-1}(A))<-R$. In all four cases we get the inequality

$$R^3-\alpha^2R-(1-\beta)R>0.$$

This inequality holds for all $R>\sqrt{\alpha^2+\beta+1}$.

Let $\beta<0$ and $R>R_0=\sqrt{\alpha^2+1-\beta}$. Consider a point $p\in M_1(R)$, and the vertical line segment V_p with $x=\pi_1(p)$ and $|y|\leq R$. The set $F_{\alpha,\beta}(V_p)$ is a horizontal line segment on the line $y=\pi_1(p)$, and since $F_{\alpha,\beta}(M_1(R))\subset$ int $(M_1(R)$ we have $\pi_1(\min(V_p))>\pi_1(p)$. Hence $\pi_1(p)<\pi_1(F_{\alpha,\beta}(p))$, and lemma 5 implies that $\mathbf{\Omega}(F_{\alpha,\beta})\cap M_1(R)=\varnothing$. By similar arguments we see that $\mathbf{\Omega}(F_{\alpha,\beta})\cap M_2(R)=\varnothing$, $\mathbf{\Omega}(F_{\alpha,\beta})\cap M_3(R)=\mathbf{\Omega}(F_{\alpha,\beta}^{-1})\cap M_3(R)=\varnothing$ and $\mathbf{\Omega}(F_{\alpha,\beta})\cap M_3(R)=\mathbf{\Omega}(F_{\alpha,\beta}^{-1})\cap M_4(R)=\varnothing$.

If $\beta>0$ and $R>R_0=\sqrt{\alpha^2+1+\beta}$ we find by the same arguments as above that $\mathbf{\Omega}(F_{\alpha,\beta})\cap M_1(R)=\varnothing$ and $\mathbf{\Omega}(F_{\alpha,\beta})\cap M_2(R)=\varnothing$. The inclusions $F_{\alpha,\beta}^{-1}(M_2(R))\subset$ int $(M_4(R)$ and $F_{\alpha,\beta}^{-1}(M_4(R))\subset$ int $(M_2(R)$ imply that $F_{\alpha,\beta}^{-2}(M_2(R))\subset$ int $(M_2(R)$ and $F_{\alpha,\beta}^{-2}(M_4(R))\subset$ int $(M_4(R)$. Consider a point $p\in M_2(R)$, and the horizontal line segment H_p with $y=\pi_2(p)$ and $|x|\leq R$. $F_{\alpha,\beta}^{-1}(H_p)$ is a vertical line segment on the line $x=\pi_2(p)$ with $\max(\pi_2(F_{\alpha,\beta}^{-1}(H_p)))<-\pi_2(p)$. The image of the vertical segment is a qubic curve segment, and since $F_{\alpha,\beta}^{-1}(M_4(R))\subset$ int $(M_2(R)$ we see that $\pi_2(F_{\alpha,\beta}^{-1}(F_{\alpha,\beta}^{-1}(H_p)))>\pi_2(p)$. Then by lemma 5 we find that $\mathbf{\Omega}(F_{\alpha,\beta})\cap M_2(R)=\mathbf{\Omega}(F_{\alpha,\beta}^{-1})\cap M_2(R)=\mathbf{\Omega}(F_{\alpha,\beta}^{-2})\cap M_2(R)=\varnothing$. By a similar argument we find that $\mathbf{\Omega}(F_{\alpha,\beta})\cap M_4(R)=\varnothing$.

The above arguments show that $\mathbf{\Omega}(F_{\alpha,\beta})\subset$ int $(\mathcal{S}(R))$ for any $R>\sqrt{\alpha^2+1+|\beta|}$.

THE NON-WANDERING SET OF THE LIFTED SYSTEM FOR $0\leq\alpha(\beta)<\sqrt{1-\beta}$. Let p_1, p_2 and p_3 denote the fixed points of $F_{\alpha,\beta}$ as above. For $0\leq\alpha(\beta)<\sqrt{1-\beta}$ all fixed points are hyperbolic. Let $W^s(p_i,F_{\alpha,\beta})$ denote the stable manifold and $W^u(p_i,F_{\alpha,\beta})$ the unstable manifold of p_i, $i=1,2,3$. If $0\leq\alpha(\beta)<\sqrt{1-\beta}$ then $\dim(W^s(p_2,F_{\alpha,\beta}))=2$. The stable manifold theorem [P&M] gives that $W^s(p_2,F_{\alpha,\beta})$ is an injectively immersed copy of $\mathbb{R}^2$. There are two cases to consider; $W^s(p_2,F_{\alpha,\beta})$ is contained in a compact set or $W^s(p_2,F_{\alpha,\beta})$ is unbounded.

Suppose $W^s(p_2, F_{\alpha,\beta})$ is contained in some compact set. Then $\mathrm{cl}(W^s(p_2, F_{\alpha,\beta}))$ is invariant and is a closed topological disc. Clearly the set $\mathrm{cl}(W^s(p_2, F_{\alpha,\beta})) \setminus W^s(p_2, F_{\alpha,\beta})$ is an invariant simple closed curve, but this is impossible since $F_{\alpha,\beta}$ contracts area for $0 < |\beta| < 1$. We conclude that $W^s(p_2, F_{\alpha,\beta})$ is unbounded.

Let $\mathcal{S}(R)$ be as in the previous section with vertices A, B , C and D. Let $R = \sqrt{\alpha^2 + 1 + |\beta|}$. Then $\mathbf{\Omega}(F_{\alpha,\beta}) \subset \mathcal{S}(R)$. Since $W^s(p_2, F_{\alpha,\beta})$ is unbounded it intersects the boundary of $\mathcal{S}(R)$. Now, $F_{\alpha,\beta}(M_i(R)) \subset M_i(R)$, $i = 1, 3$, so $W^s(p_2, F_{\alpha,\beta})$ can not intersect the line segments BC and AD. By the symmetry $F_{\alpha,\beta}(-x, -y) = -F_{\alpha,\beta}(x, y)$ it follows that $W^s(p_2, F_{\alpha,\beta})$ intersects both linesegments AB and CD. By the same reason as above we see that $W^s(p_i, F_{\alpha,\beta}) \cap (\mathrm{int}\ (M_1(R)) \cup \mathrm{int}\ (M_3(R))) = \varnothing$, $i = 1, 3$, and since $F^{-1}_{\alpha,\beta}(M_2(R) \cup M_4(R)) \subset M_2(R) \cup M_4(R)$ we see that $W^u(p_i, F_{\alpha,\beta}) \cap (\mathrm{int}\ (M_2(R)) \cup \mathrm{int}\ (M_4(R))) = \varnothing$ for $i = 1, 3$.

We claim that $W^s(p_i, F_{\alpha,\beta}) \subset \mathrm{cl}(()W^s(p_2, F_{\alpha,\beta}))$, $i = 1, 3$. If this is the case it is easily seen by the λ-lemma [P&M] that $\mathbf{\Omega}(F_{\alpha,\beta}) \cap \mathcal{S}(R) = \{p_1, p_2, p_3\}$, and hence $\mathbf{\Omega}(F_{\alpha,\beta}) = \{p_1, p_2, p_3\}$.

To prove this claim it is sufficient, by the λ-lemma, to show that $W^s(p_2, F_{\alpha,\beta}) \cap W^u(p_i, F_{\alpha,\beta}) \neq \varnothing$, $i = 1, 3$. By symmetry this reduces to show that $W^s(p_2, F_{\alpha,\beta}) \cap W^u(p_3, F_{\alpha,\beta}) \neq \varnothing$.

Let $\tilde{\mathcal{S}}(R)$ be the square with vertices $(0, 0)$, $(R, 0)$, (R, R) and $(0, R)$. $W^u(p_3, F_{\alpha,\beta})$ is an injectively immersed copy of $\mathbb{R}$, and from the eigenvalues of the Jacobi matrix of $F_{\alpha,\beta}$ at p_3 it follows that $F_{\alpha,\beta}|_{W^u(p_3, F_{\alpha,\beta})}$ is orientation preserving. It is also clear by the geometric properties of $F_{\alpha,\beta}$ that a part of $W^u(p_3, F_{\alpha,\beta})$ is contained in $M_1(R)$. Let

$$K = \bigcap_{n=0}^{\infty} F^n_{\alpha,\beta}(\tilde{\mathcal{S}}(R)).$$

Then $K \supset \{p_2, p_3\}$ and K must contain a part of $W^u(p_3, F_{\alpha,\beta})$. K is a curve segment, and since $F_{\alpha,\beta}|_{W^u(p_3, F_{\alpha,\beta})}$ is orientation preserving we see that the segment of K with endpoints p_2 and p_3 is invariant. Let $K' = [p_1, p_2] \subset K$. Let $p \in K' \cap W^u_{loc}(p_3, F_{\alpha,\beta})$, $p \neq p_3$. By invariance of K' we see that the ω-limit of p is in K', and since $F_{\alpha,\beta}|_{W^u(p_3, F_{\alpha,\beta})}$ is orientation preserving $\omega(p, F_{\alpha,\beta})$ must be a fixed point. Hence $\omega(p, F_{\alpha,\beta}) = p_2$, so $W^u(p_3, F_{\alpha,\beta}) \cap W^s(p_2, F_{\alpha,\beta}) \neq \varnothing$.

The above shows that if $W^s(p_2, F_{\alpha,\beta})$ is two dimensional, and p_1 and p_3 hyperbolic saddles then $\mathbf{\Omega}(F_{\alpha,\beta}) = \{p_1, p_2, p_3\}$, This is the case when $0 \leq \alpha(\beta) < \alpha_0(\beta) = \sqrt{1 - \beta}$. For $\alpha(\beta) > \alpha_0(\beta)$ the non-wandering set of $F_{\alpha,\beta}$ becomes more and more complex for increasing $\alpha(\beta)$.

TOPOLOGICAL HORSESHOES IN THE LIFTED SYSTEM. Suppose $\beta > 0$. Consider the square $\mathcal{S}(R) = [-R, R] \times [-R, R]$ with vertices $A = (-R, -R)$, $B = (R, -R)$, $C = (R, R)$ and $D = (-R, R)$. The linesegments AB and CD are mapped to qubic curvesegments, and the linesegments BC and AD are mapped to horizontal linesegments. If R is large enough the qubic segments have both a minimum and a maximum in the first coordinate in in the interior of $[-R, R]$. A calculation shows that the minimum is obtained in the image of the points $(\alpha/\sqrt{3}, \pm R)$ and that maximum is obtained in the image of the points $(-\alpha/\sqrt{3}, \pm R)$. Let $m = (-\alpha/\sqrt{3}, -R)$. By symmetry we see that if

$$\pi_1(F_{\alpha,\beta}(D)) < -R \quad \text{and} \quad \pi_1(F_{\alpha,\beta}(m)) > R \tag{4}$$

then $\mathcal{S}(R) \cap F_{\alpha,\beta}(\mathcal{S}(R))$ consists of three horizontal strips cutting through $\mathcal{S}(R)$, that is, the endpoints of the strips intersect the interior of the linesegments BC and AD. $\pi_1(F_{\alpha,\beta}(D)) < -R$ gives $R > \sqrt{\alpha^2 + \beta + 1}$ and $\pi_1(F_{\alpha,\beta}(m)) > R$ gives $R < \frac{2\alpha^3}{3\sqrt{3}(\beta+1)}$. $\frac{2\alpha^3}{3\sqrt{3}(\beta+1)}$ grows much faster than $\sqrt{\alpha^2 + \beta + 1}$, and therefore there exists an $\alpha_1(\beta)$ such that (4) holds for $\sqrt{\alpha^2 + \beta + 1} < R < \frac{2\alpha^3}{3\sqrt{3}(\beta+1)}$. This α-value is found by solving the equation

$$\sqrt{\alpha^2 + \beta + 1} = \frac{2\alpha^3}{3\sqrt{3}(\beta + 1)}.$$

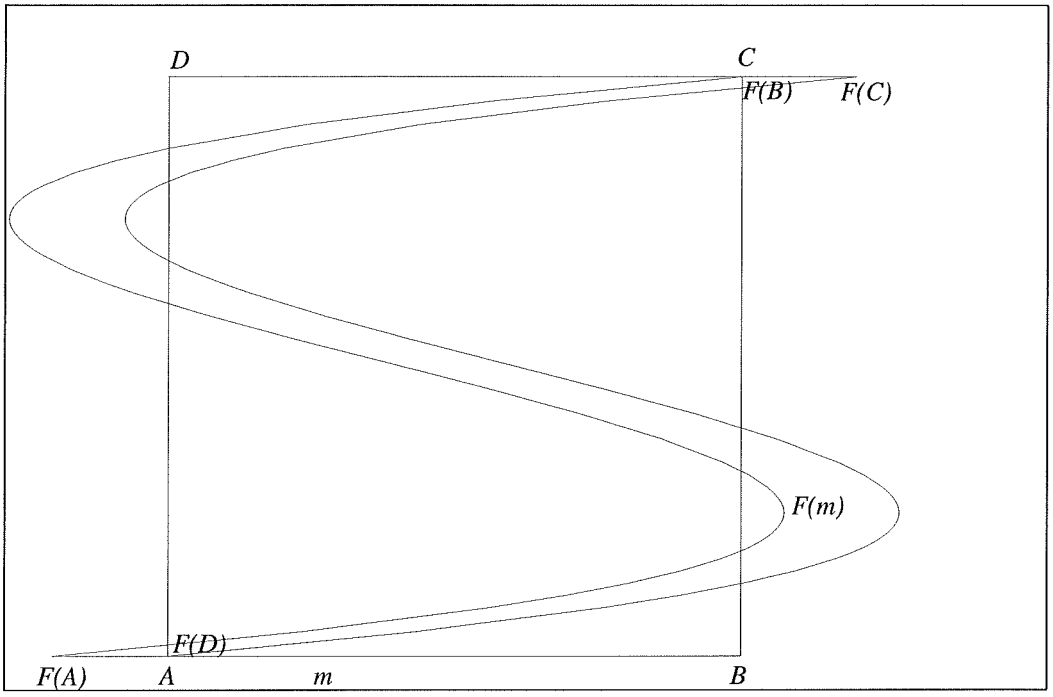

FIGURE 1.7.
The image of the square $[-R, R] \times [-R, R]$ for $\alpha = 2.0$, $\beta = 0.2$ and $R = 2.281$. We note that $\alpha_1(0.2) \approx 1.8974$.

By squaring the equation we obtain

$$4\alpha^6 - 27(\beta+1)^2\alpha^2 - 27(\beta+1)^3 = 0.$$

This equation is of the form $4\gamma^3 - 27\eta^2\gamma - 27\eta^3 = 0$. It is easily seen that this equation has a unique real root γ_0 for $\gamma \geq 0$ and this root is of the form $\gamma_0 = k\eta$ where $k^3 - 27k - 27 = 0$, and therefore $k = 3$. Hence $\gamma_0 = 3\eta$. By substituting this in the definitions of γ and η and using the fact that $\alpha \geq 0$ we find that $\alpha_1(\beta) = \sqrt{3(1+\beta)}$. A similar calculation with $F^{-1}_{\alpha,\beta}$ gives of course the same result.

The same calculation for $\beta < 0$ with the conditions $\pi_1(F_{\alpha,\beta}(A)) < -R$ and $\pi_1(F_{\alpha,\beta}(\tilde{m})) > R$, where $\tilde{m} = (-\alpha/\sqrt{3}, R)$, gives $\alpha_1(\beta) = \sqrt{3(1-\beta)}$.

From the previous we know that $\mathbf{\Omega}(F_{\alpha,\beta}) \subset \mathcal{S}(R)$, and the maximal invariant set in $\mathcal{S}(R)$ is given by

$$\Lambda(F_{\alpha,\beta}) = \bigcap_{n=-\infty}^{\infty} F^n_{\alpha,\beta}(\mathcal{S}(R)).$$

By the construction we see that

$$H_n = \bigcap_{i=0}^{n} F^i_{\alpha,\beta}(\mathcal{S}(R)) \text{ and } V_n = \bigcap_{i=0}^{n} F^{-i}_{\alpha,\beta}(\mathcal{S}(R))$$

consist of 3^n horizontal strips and 3^n vertical strips respectively. Clearly the vertical size of each strip in H_n, and the horizontal size of each strip in V_n approaches 0 at least as fast as $2R/3^n$, so

$$H_\infty = \bigcap_{i=0}^{\infty} F^i_{\alpha,\beta}(\mathcal{S}) \text{ and } V_\infty = \bigcap_{i=0}^{\infty} F^{-i}_{\alpha,\beta}(\mathcal{S})$$

are unions of horizontal curves and vertical curves respectively, such that $l_h \in H_\infty$ and $l_v \in V_\infty$ intersects in a unique point. Let $\Lambda(F_{\alpha,\beta}) = V_\infty \cap H_\infty$. We construct a homeomorphism $h : \Lambda(F_{\alpha,\beta}) \longrightarrow \Sigma_3$ as in [G&H] such that the diagram

$$\begin{array}{ccc} \Lambda(F_{\alpha,\beta}) & \xrightarrow{F_{\alpha,\beta}} & \Lambda(F_{\alpha,\beta}) \\ {\scriptstyle h}\downarrow & & \downarrow{\scriptstyle h} \\ \Sigma_3 & \xrightarrow{\sigma} & \Sigma_3 \end{array}$$

commutes. The periodic points are dense in Σ_3, and $\Lambda(F_{\alpha,\beta})$ is the largest invariant set in $\mathcal{S}(R)$, so $\mathbf{\Omega}(F_{\alpha,\beta}) = \Lambda(F_{\alpha,\beta})$.

The above arguments show that $F_{\alpha,\beta}$ restricted to $\mathbf{\Omega}(F_{\alpha,\beta})$ is topologically equivalent to a full shift on three symbols for all $\alpha(\beta) > \alpha_1(\beta) = \sqrt{3(1+|\beta|)}$, and $\beta \neq 0$.

HYPERBOLIC HORSESHOES IN THE LIFTED SYSTEM. Suppose $\beta > 0$. Let $\mathcal{S}(R)$ be as above with $R = \sqrt{\alpha^2+1+\beta}$, and $\alpha(\beta) > \sqrt{3(1+\beta)}$. $F_{\alpha,\beta}(\mathcal{S}(R)) \cap \mathcal{S}(R)$ consists of three horizontal strips cutting through $\mathcal{S}(R)$. We denote these strips by $\mathcal{H}_i$, $i = 1,2,3$. These strips are contained in three horizontal rectangles $\mathcal{R}_i$, $i = 1,2,3$.

We want to find the vertices of $\mathcal{R}_i$. The image of the line segment AB intersect the line segment BC in three points, (R, y_1), (R, y_2) and (R, R) where $y_1 < y_2 < 0$. By the symmetric properties of $F_{\alpha,\beta}$ we see that (we give only the lower left and upper right vertex) the vertices of $\mathcal{R}_1$ are $(-R, R)$ and (R, y_1), $(-R, y_2)$ and $(R, -y_2)$ for $\mathcal{R}_2$ and $(-R, -y_1)$ and (R, R) for $\mathcal{R}_3$. The points y_1 and y_2 are solutions of $y^3 - \alpha^2 y - \beta R = R$. Since $y = R$ solves this equation we see that $y^3 - \alpha^2 y - (\beta+1)R = (y^2 + Ry + R^2 - \alpha^2)(y - R)$ so

$$y_1 = -\frac{1}{2}\left(R + \sqrt{4\alpha^2 - 3R^2}\right) = -\frac{1}{2}\left(\sqrt{\alpha^2+1+\beta} + \sqrt{\alpha^2 - 3(1+\beta)}\right)$$
$$y_2 = -\frac{1}{2}\left(R - \sqrt{4\alpha^2 - 3R^2}\right) = -\frac{1}{2}\left(\sqrt{\alpha^2+1+\beta} - \sqrt{\alpha^2 - 3(1+\beta)}\right).$$

Similar $F^{-1}_{\alpha,\beta}(\mathcal{S}(R)) \cap \mathcal{S}(R)$ consists of three vertical strips cutting through $\mathcal{S}(R)$. These strips are contained in rectangles $\mathcal{P}_i$, $i = 1,2,3$. The vertices of these rectangles are the same as for the rectangles $\mathcal{R}_i$ with the x- and y-coordinate interchanged.

We remark that $y_2 - y_1 = \sqrt{\alpha^2 - 3(1+\beta)}$ is an increasing function in α, and that simple calculations show that $\frac{\partial y_1}{\partial \alpha} < 0$ and $\frac{\partial y_2}{\partial \alpha} > 0$.

We will now use lemma 9 to obtain hyperbolicity conditions; let $t = 3x^2 - \alpha^2$, $s = \beta$ and $k = l = 1$ in lemma 9. By the symmetric properties of $F_{\alpha,\beta}$ it is sufficient to choose $\alpha(\beta)$ such that

$$3y_1^2 - \alpha^2 > 1 + \beta$$

and

$$3y_2^2 - \alpha^2 < -(1+\beta).$$

After some calculations we find that $3y_1^2 - \alpha^2 = 1+\beta$ reduces to $2\alpha^4 - 2(1+\beta)\alpha^2 - 13(1+\beta)^2 = 0$. This equation has positive solution

$$\alpha_{21}(\beta) = \sqrt{\frac{1+\sqrt{27}}{2}}\sqrt{1+\beta}.$$

The equation $3y_2^2 - \alpha^2 = -(1+\beta)$ reduces to $2\alpha^4 - 8(1+\beta)\alpha^2 - 7(1+\beta)^2 = 0$, with positive solution

$$\alpha_{22}(\beta) = \sqrt{\frac{4+\sqrt{30}}{2}}\sqrt{1+\beta}.$$

Lemma 9, the theorem from [New] in section 1, the previous section and the monotone properties of y_1 and y_2 implies that $\mathbf{\Omega}(F_{\alpha,\beta}) \simeq \Sigma_3$ has a hyperbolic structure for

$$\alpha(\beta) > \alpha_2(\beta) = \max\{\alpha_{21}(\beta), \alpha_{22}(\beta)\} = \sqrt{\frac{4+\sqrt{30}}{2}}\sqrt{1+\beta} \quad \text{if} \quad \beta > 0.$$

A similar argument for $\beta < 0$ show that $\mathbf{\Omega}(F_{\alpha,\beta}) \simeq \Sigma_3$ has a hyperbolic structure for $\alpha(\beta) > \alpha_2(\beta)$ where

$$\alpha_2(\beta) = \sqrt{\frac{4+\sqrt{30}}{2}}\sqrt{1-\beta}.$$

These arguments show that $\mathbf{\Omega}(F_{\alpha,\beta}) \simeq \Sigma_3$, $\beta \neq 0$, has a hyperbolic structure for $\alpha(\beta) > \alpha_2(\beta)$ where

$$\alpha_2(\beta) = \sqrt{\frac{4+\sqrt{30}}{2}}\sqrt{1+|\beta|}.$$

Remark. The one-dimensional system has a one-sided hyperbolic 3-shift for $\alpha > \sqrt{\frac{1+3\sqrt{3}}{2}}$. We see that

$$\alpha_2(0) = \sqrt{\frac{4+\sqrt{30}}{2}} > \sqrt{\frac{1+3\sqrt{3}}{2}}.$$

The reason for this disagreement is the same as given in the remark after theorem 4, since $\alpha_2(\beta)$ is an upper bound, and $\alpha = \sqrt{\frac{1+3\sqrt{3}}{2}}$ is the smallest α-value such that the one-dimensional system has a hyperbolic one sided 3-shift.

References

[A1] Stephen A. Andrea, *On homeomorphisms of the plane, and their embeddings in flows*, Bull. Amer. Math. Soc. **71** (1965), 381–383.

[A2] Stephen A. Andrea, *On homeomorphisms of the plane which have no fixed points*, Abh. Math. Sem. Univ. Hamburg **30** (1967), 61–74.

[Dev] Robert L. Devaney, *An Introduction to Chaotic Dynamical Systems*, The Benjamin/Cummnings Publishing Co. Inc., 1986.

[G&H] John Guckenheimer and Philip Holmes, *Nonlinear Oscillations, Dynamical Systems, and Bifurcations of Vector Fields*, Springer-Verlag, 1983.

[K&K&Y] Ittai Kan, Hüseyin Koçak and James A. Yorke, *Antimonotonicity: Concurrent creation and annilation of periodic orbits*, Annals of Mathematics **136** (1992), 219–252.

[New] Sheldon Newhouse, *Lectures on dynamical systems*, Dynamical systems (1980), Birkhäuser.

[P&M] Jacob Palis, Jr. and Welington de Melo, *Geometric Theory of Dynamical Systems*, Springer-Verlag, 1982.

Department of Mathematics, University of Oslo, P.O. Box 1053 Blindern, N-0316 Oslo
E-mail address: tojonass@math.uio.no